Classical and Quantum Gravity

PAPER • OPEN ACCESS

Extraction of gravitational-wave energy in higher dimensional numerical relativity using the Weyl tensor

To cite this article: William G Cook and Ulrich Sperhake 2017 *Class. Quantum Grav.* **34** 035010

OPEN ACCESS
IOP Publishing
Classical and Quantum Gravity
Class. Quantum Grav. **34** (2017) 035010 (31pp)
doi:10.1088/1361-6382/aa5294

Extraction of gravitational-wave energy in higher dimensional numerical relativity using the Weyl tensor

William G Cook[1] **and Ulrich Sperhake**[1,2,3]

[1] Department of Applied Mathematics and Theoretical Physics, Centre for Mathematical Sciences, University of Cambridge, Wilberforce Road, Cambridge CB3 0WA, UK
[2] Department of Physics and Astronomy, The University of Mississippi, University, MS 38677-1848, USA
[3] Theoretical Astrophysics 350-17, California Institute of Technology, Pasadena, CA 91125, USA

E-mail: wc259@damtp.cam.ac.uk

Received 2 September 2016, revised 10 November 2016
Accepted for publication 8 December 2016
Published 9 January 2017

Abstract

Gravitational waves are one of the most important diagnostic tools in the analysis of strong-gravity dynamics and have been turned into an observational channel with LIGO's detection of GW150914. Aside from their importance in astrophysics, black holes and compact matter distributions have also assumed a central role in many other branches of physics. These applications often involve spacetimes with $D > 4$ dimensions where the calculation of gravitational waves is more involved than in the four dimensional case, but has now become possible thanks to substantial progress in the theoretical study of general relativity in $D > 4$. Here, we develop a numerical implementation of the formalism by Godazgar and Reall [1]—based on projections of the Weyl tensor analogous to the Newman–Penrose scalars—that allows for the calculation of gravitational waves in higher dimensional spacetimes with rotational symmetry. We apply and test this method in black-hole head-on collisions from rest in $D = 6$ spacetime dimensions and find that a fraction $(8.19 \pm 0.05) \times 10^{-4}$ of the Arnowitt–Deser–Misner mass is radiated away from the system, in excellent agreement with literature results based on the Kodama–Ishibashi perturbation technique. The method presented here complements the perturbative approach by automatically including contributions from all multipoles rather than computing the energy content of individual multipoles.

Keywords: gravitational waves, black holes, higher dimensions

(Some figures may appear in colour only in the online journal)

1. Introduction

Gravitational waves (GWs) entered the limelight with the recent detection of GW150914 [2]—soon followed by a second detection GW151226 [3]—which not only constitutes the first observation of a black-hole (BH) binary system, but also marks a true milestone in gravitational physics. This breakthrough has opened a qualitatively new path for measuring BH parameters [4, 5], testing Einstein's theory of general relativity [6] and probing extreme astrophysical objects and their formation history [7], and substantially broadens the scope of multi-messenger astronomy [8]. GW modelling, however, finds important applications beyond the revolutionary field of GW astronomy. Many fundamental questions in general relativity in $D = 4$ and $D > 4$ spacetime dimensions concern the stability of strong-gravity sources (see [9–16] and references therein) in the context of cosmic censorship violation, the solutions' significance as physical objects or expanding our understanding of the strong-field regime of general relativity. For instance, GW extraction from numerical simulations of rapidly spinning Myers–Perry BHs demonstrates how excess angular momentum is shed in order to allow the BH to settle down into a more slowly rotating configuration [13]. GW emission also represents a channel for mass-energy loss in ultra-relativistic collisions that are studied in the context of the so-called TeV gravity scenarios that may explain the hierarchy problem in physics; for reviews see e.g. [17–19].

The calculation of GW signals in the theoretical modelling of $D = 4$ dimensional sources in the framework of general relativity has been increasingly well understood following seminal work by Pirani, Bondi, Sachs and others in the 1950s and 1960s; see e.g. [20–26] and [27] for a review. Applications are now routinely found in numerical and (semi-)analytic calculations [28–37] even though care needs to be taken when applied to numerical simulations on finite domains [38].

The numerical study of solutions to Einstein's equations has proven incredibly useful for understanding the behaviour of black holes and other compact objects. Most recently, the application of numerical relativity in the generation of gravitational waveform templates for GW data analysis [37, 39–44] contributed to the above mentioned detection of GW150914.

The wave extraction techniques presently used in numerical simulations of astrophysical GW sources can be classified as follows: perturbative methods based on the formalism developed by Regge, Wheeler, Zerilli and Moncrief [9, 10, 45]; application of the quadrupole formula [46] in matter simulations [47, 48]; a method using the Landau–Lifshitz pseudo-tensor [49, 50] ; Cauchy characteristic extraction [51–53]; and, probably the most popular technique, using the Weyl scalars from the Newman–Penrose formalism [24, 54–60]. A comparison of various of these techniques is given in [36] and an extended review in [61].

The calculation of GWs in higher dimensional relativity requires generalisation of these techniques to $D > 4$. The extraction of the GW energy flux from the Landau–Lifshitz pseudo-tensor has been generalised straightforwardly to higher dimensions in [62, 63]. An extension of the Regge–Wheeler–Zerilli–Moncrief formalism for perturbations of spherically symmetric background spacetimes is available in the form of the Kodama and Ishibashi (KI) formalism [64, 65] and forms the basis of the wave extraction techniques developed in [66, 67]. The main assumption there is that far away from the strong-field regime, the spacetime is perturbatively close to the Tangherlini [68] spacetime. The deviations from this background facilitate the construction of master functions according to the KI formalism which in turn provide

the energy flux in the different (l,m) radiation multipoles. Even though both methods are in practice applied at finite extraction radius, their predictions have been found to agree within a $\sim$1% error tolerance when applied to BH head-on collisions starting from rest in $D = 5$ [69]. Recent years have also seen considerable progress in the understanding of the peeling properties of the Weyl tensor; see [1, 70] and references therein.

In particular, Godazgar and Reall [1] have performed a decomposition of the Weyl tensor in higher dimensions, and derived a generalisation of the Newman–Penrose formalism for wave extraction to $D > 4$. This analysis provides us with a quantity analogous to the Weyl scalar Ψ_4, from which we can calculate the energy radiated in gravitational waves in a similar fashion to the method in $D = 4$. The one qualitative difference between the $D = 4$ and $D > 4$ cases comes in the availiability of a mode decomposition of the gravitational wave. In $D = 4$ we can project the Weyl scalar onto spin weighted spherical harmonics, due to the decoupling of the equations of motion as shown by Teukolsky [71, 72]. In higher dimensions however, a set of conditions identified as sufficient for decoupling are not satisfied in black hole spacetimes [73], and so at present we are unable to project out the angular dependence of the gravitational wave energy. The numerical implementation of this formalism and probing the accuracy for a concrete example application is the subject of this paper.

For this purpose, we require a formulation of the higher dimensional Einstein equations suitable for numerical integration. For computational practicality, all higher dimensional time evolutions in numerical relativity have employed symmetry assumptions to reduce the problem to an effective '$d + 1$' dimensional computation where typically $d \leqslant 3$. This has been achieved in practice by either (i) imposing the symmetries directly on the metric line element [74], (ii) dimensional reduction by isometry of the Einstein field equations [75, 76] or (iii) use of so-called *Cartoon* methods [13, 77–80]. In our implementation, we use the latter method combined with the Baumgarte–Shapiro–Shibata–Nakamura [81, 82] (BSSN) formulation of the Einstein equations as expanded in detail in [83]. The relevant expressions for the GW computation, however, will be expressed in terms of the Arnowitt–Deser–Misner [84] (ADM) variables, and the formalism as presented here can be straightforwardly applied in other common evolution systems used in numerical relativity.

The paper is structured as follows. In section 2 we describe the notation used in the remainder of this work. In section 3 we recapitulate the key results of [1] which sets up the formalism. In section 4 we put the formalism into a form compatible with the modified Cartoon dimensional reduction of our simulations. In section 5 we describe the numerical set up used in our simulations, analyse the energy radiated in BH collisions in $D = 6$ and compare the predictions with literature results based on alternative wave extraction techniques.

2. Notation and indices

The key goal of our work is to extract the GW signal from dynamical, asymptotically flat D dimensional spacetimes, i.e. manifolds $\mathcal{M}$ equipped with a metric g_{AB}, $A, B = 0, \ldots, D-1$, of signature $D - 2$ that obey the Einstein equations with vanishing cosmological constant

$$G_{AB} = R_{AB} - \frac{1}{2} R g_{AB} = 8\pi T_{AB}. \tag{2.1}$$

Here, T_{AB} is the energy momentum tensor which we assume to vanish in the wave zone, R_{AB} and R denote the Ricci tensor and scalar, respectively, and we are using units where the gravitational constant and the speed of light $G = c = 1$. Furthermore, we define the Riemann tensor and Christoffel symbols according to the conventions of Misner, Thorne and Wheeler [85].

The ADM space-time decomposition as reformulated by York [86] writes the metric line element in the form

$$ds^2 = g_{AB}dx^A dx^B = (-\alpha^2 + \beta_I\beta^I)dt^2 + 2\beta_I dx^I dt + \gamma_{IJ}dx^I dx^J, \tag{2.2}$$

where $I, J = 1, \ldots, D-1$, α and β^I denote the lapse function and shift vector, respectively, and γ_{IJ} is the spatial metric that determines the geometry of hypersurfaces $t = \text{const}$. For this choice of coordinates and variables, the Einstein equations (2.1) result in one *Hamiltonian* and $D-1$ *momentum* constraints as well as $D(D-1)/2$ evolution equations cast into first-order-in-time form by introducing the extrinsic curvature K_{IJ} through

$$\partial_t \gamma_{IJ} = \beta^M \partial_M \gamma_{IJ} + \gamma_{MJ}\partial_I \beta^M + \gamma_{IM}\partial_J \beta^M - 2\alpha K_{IJ}\,; \tag{2.3}$$

for a detailed review of this decomposition see [87, 88].

In the remainder of this work we assume that the ADM variables are available. The BSSN formulation, for example, employs a conformally rescaled spatial metric $\tilde{\gamma}_{IJ}$, the rescaled traceless extrinsic curvature $\tilde{A}_{IJ}$, a conformal factor χ, the trace of the extrinsic curvature K and contracted Christoffel symbols $\tilde{\Gamma}^I$ associated with the conformal metric. These are related to the ADM variables by

$$\begin{aligned}
&\chi = \gamma^{-1/(D-1)}, \gamma = \det\gamma_{IJ}, && K = \gamma^{MN}K_{MN}, \\
&\tilde{\gamma}_{IJ} = \chi\gamma_{IJ} && \Leftrightarrow\quad \tilde{\gamma}^{IJ} = \frac{1}{\chi}\gamma^{IJ}, \\
&\tilde{A}_{IJ} = \chi\left(K_{IJ} - \frac{1}{D-1}\gamma_{IJ}K\right) && \Leftrightarrow\quad K_{IJ} = \frac{1}{\chi}\left(\tilde{A}_{IJ} + \frac{1}{D-1}\tilde{\gamma}_{IJ}K\right), \\
&\tilde{\Gamma}^I = \tilde{\gamma}^{MN}\tilde{\Gamma}^I_{MN}, &&
\end{aligned} \tag{2.4}$$

so that the ADM variables can be reconstructed straightforwardly at every time in the evolution. For other popular evolution systems such as the conformal Z4 system [89–91] or the generalised harmonic formulation [77, 92] the ADM variables are obtained in similar fashion or directly from the spacetime metric components through equations (2.2) and (2.3).

Many practical applications of higher dimensional numerical relativity employ symmetry assumptions that reduce the computational domain to an effective three dimensional spatial grid using the aforementioned techniques. The reasons are two-fold: (i) the computational cost of simulations in $D > 3+1$ dimensions massively increases with any dimension added and (ii) the $SO(D-d)$ rotational symmetry accommodates many applications of interest that can therefore be handled by relatively straightforward extensions of numerical codes originally developed for astrophysical systems in four spacetime dimensions. The so-called *cartoon methods* have been developed for this specific purpose. An illustration of the idea is given in figure 1, where rotational symmetry is assumed in every plane spanned by two of the coordinates (z, w^a), where $a = d+1, \ldots, D-1$. Knowledge of the tensorial components in the d dimensional hypersurface spanned by $(x^{\hat{i}}, z)$, $\hat{i} = 1, \ldots, d-1$ then is sufficient to describe the entire spacetime. In numerical evolutions, however, there remains the question of evaluating derivatives perpendicular to that plane. In the original cartoon version [93], this was achieved through ghost zones off the computational domain which are populated by rotation of the data on the plane and then facilitate evaluation of the derivatives through standard discretisation methods. A modification of this method introduced in [77] (see also [13, 79, 80]), dispenses with the need for ghost zones. Instead, the required derivatives are obtained through analytic relations from derivatives in the on-domain directions. A detailed discussion and some example cases for the derivation of these relations are given in [83].

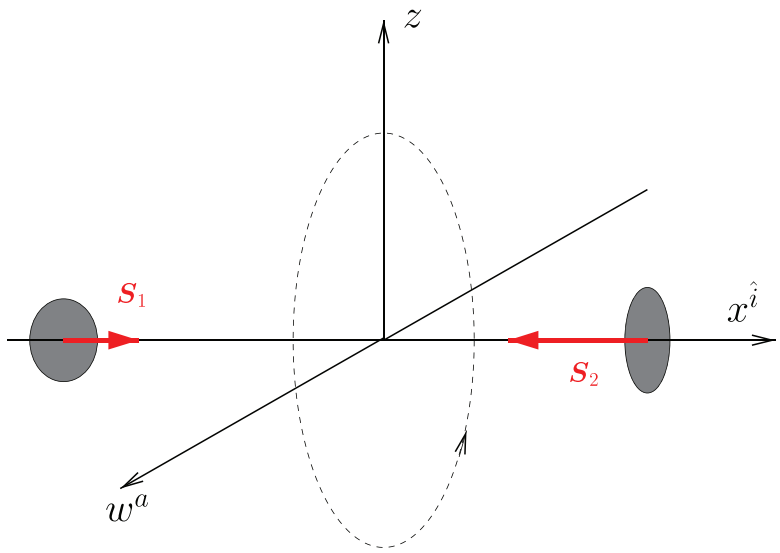

Figure 1. Illustration of the cartoon method. The $D-1$ dimensional spatial domain is represented by $D-1$ Cartesian coordinates $x^{\hat{i}}$, z and w^a where $\hat{i}=1,\ldots,d-1$, $a=d+1,\ldots,D-1$ and d is the number of effective dimensions of the computational domain. Rotational symmetry is assumed in all planes spanned by two of the (z, w^a). For example, collisions of black holes in the $x^{\hat{i}}$ plane, possibly with spin $\boldsymbol{S}$ inside this plane, can be modelled this way.

In general, this method reduces the number of effective (spatial) dimensions from $D-1$ to d, where $1\leqslant d\leqslant D-2$. $d=1$ corresponds to spherical symmetry, i.e. $SO(D-1)$ isometry, and the other extreme $d=D-2$ corresponds to the axisymmetric case $SO(2)$ with rotational symmetry about one axis. As already detailed in [83], axisymmetry represents a special case that imposes fewer constraints on the components of tensors and their derivatives and is therefore most conveniently handled numerically in a manner similar but not identical to the general case. We will discuss first in detail the case $1\leqslant d\leqslant D-3$ and then describe the specific recipe for dealing with $d=D-2$. Probably the most important situation encountered in practical applications is that of an effective $d=3$ dimensional spatial computational domain. Whenever the expressions developed in the remainder of this work for general d are not trivially converted to $d=3$, we shall explicitly write down the $d=3$ version in addition to the general case.

Let us start by considering a spacetime with at least two rotational Killing vectors which is the scenario discussed in sections 2 and 3 of [83]. For convenience, we will employ two specific coordinate systems adapted to this situation. The first is a set of Cartesian coordinates

$$X^A=(t,\underbrace{x^1,\ldots,x^{d-1}}_{(d-1)\times},z,\underbrace{w^{d+1},\ldots,w^{D-1}}_{(D-d-1)\times})=(t,x^{\hat{i}},z,w^a)=(t,x^i,w^a), \tag{2.5}$$

where middle Latin indices without (with) a caret range from $i=1,\ldots,d$ ($\hat{i}=1,\ldots,d-1$) and early Latin indices run from $a=d+1,\ldots,D-1$; see figure 1. The second is a system of spherical coordinates

$$Y^A=(t,r,\underbrace{\phi^2,\phi^3,\ldots,\phi^{D-1}}_{(D-2)\times})=(t,r,\phi^\alpha), \tag{2.6}$$

where Greek indices run from $\alpha = 2, \ldots, D-1$. We use middle, upper case Latin indices to denote all spatial coordinates of either of these systems, so that $X^I = (x^{\hat{i}}, z, w^a)$ and $Y^I = (r, \phi^\alpha)$ with $I = 1, \ldots, D-1$. Rotational symmetry is assumed in all directions ϕ^a, $a = d+1, \ldots, D-1$. In the special case $d = 3$, we use the notation $x^{\hat{i}} \equiv (x, y)$, so that equation (2.5) becomes

$$X^A = (t, x, y, z, w^4, \ldots, w^{D-1}). \tag{2.7}$$

We orient the Cartesian coordinates (2.5) such that they are related to the spherical coordinates (2.6) by

$$\begin{aligned}
(w^1 \equiv)\, x^1 &= r\cos\phi^2, \\
(w^2 \equiv)\, x^2 &= r\sin\phi^2\cos\phi^3, \\
&\vdots \\
(w^{d-1} \equiv)\, x^{d-1} &= r\sin\phi^2 \ldots \sin\phi^{d-1}\cos\phi^d, \\
(w^d \equiv)\, z &= r\sin\phi^2 \ldots \sin\phi^{d-1}\sin\phi^d\cos\phi^{d+1}, \\
w^{d+1} &= r\sin\phi^2 \ldots \sin\phi^{d-1}\sin\phi^d\sin\phi^{d+1}\cos\phi^{d+2}, \\
&\vdots \\
w^{D-3} &= r\sin\phi^2 \ldots \sin\phi^{D-3}\cos\phi^{D-2}, \\
w^{D-2} &= r\sin\phi^2 \ldots \sin\phi^{D-3}\sin\phi^{D-2}\cos\phi^{D-1}, \\
w^{D-1} &= r\sin\phi^2 \ldots \sin\phi^{D-3}\sin\phi^{D-2}\sin\phi^{D-1}.
\end{aligned} \tag{2.8}$$

Here $\phi^{D-1} \in [0, 2\pi]$, and all other $\phi^\alpha \in [0, \pi]$, and we have formally extended the w coordinates to also include (in parentheses in the equation) $w^i = x^i$ which turns out to be convenient in the notation below in section 4. Note that for the orientation chosen here, the x axis denotes the reference axis for the first polar angle rather than the z axis which more commonly plays this role for spherical coordinates in three spatial dimensions.

For orientation among the different sets of indices, we conclude this section with a glossary listing index variables and their ranges as employed throughout this work.

- Upper case early Latin indices $A, B, C, \ldots$ range over the full spacetime from 0 to $D-1$.
- Upper case middle Latin indices $I, J, K, \ldots$ denote all spatial indices, inside and outside the effective computational domain, running from 1 to $D-1$.
- Lower case middle Latin indices $i, j, k, \ldots$ denote indices in the spatial computational domain and run from 1 to d. For $d = 3$, we have $x^i = (x, y, z)$.
- Lower case middle Latin indices with a caret $\hat{i}, \hat{j}, \ldots$ run from 1 to $d-1$ and represent the x^i (without caret) excluding z. In $d = 3$, we write $x^{\hat{i}} = (x, y)$.
- Lower case early Latin indices $a, b, c, \ldots$ denote spatial indices outside the computational domain, ranging from $d+1$ to $D-1$.
- Greek indices $\alpha, \beta, \ldots$ denote all angular directions and range from 2 to $D-1$.
- Greek indices with a caret $\hat{\alpha}, \hat{\beta}, \ldots$ denote the subset of angular coordinates in the computational domain, i.e. range from 2, …, d. As before, a caret thus indicates a truncation of the index range.
- Put inside parentheses, indices cover the same range but merely denote labels rather than tensor indices.
- An index 0 denotes a contraction with the timelike normal to the foliation, rather than the time component, as detailed below in section 4.1.1.
- ∇_A denotes the covariant derivative in the full D dimensional spacetime, whereas D_I denotes the covariant derivative on a spatial hypersurface and is calculated from the spatial metric γ_{IJ}.

- We denote by R with appropriate indices the Riemann tensor (or Ricci tensor/scalar) of the full D dimensional spacetime, and by $\mathcal{R}$ the spatial Riemann tensor (or Ricci tensor/scalar) calculated from γ_{IJ}.

3. Theoretical formalism

Our wave extraction from numerical BH simulations in $D > 4$ dimensions is based on the formalism developed by Godazgar and Reall [1]. In this section, we summarise the key findings and expressions from their work.

The derivation [1] is based on the definition of asymptotic flatness using Bondi coordinates [26] $(u, \mathfrak{r}, \phi^\alpha)$ where u is retarded time, $\mathfrak{r}$ the radius and ϕ^α are $D-2$ angular coordinates covering the unit $D-2$ sphere. A spacetime is asymptotically flat at future null infinity [94] if the metric outside a cylindrical world tube of finite radius can be written in terms of functions $\mathcal{A}(u, \mathfrak{r}, \phi^\alpha)$, $\mathcal{B}(u, \mathfrak{r}, \phi^\alpha)$, $\mathcal{C}(u, \mathfrak{r}, \phi^\alpha)$ as

$$\mathrm{d}s^2 = -\mathcal{A}\mathrm{e}^{\mathcal{B}}\mathrm{d}u^2 - 2\mathrm{e}^{\mathcal{B}}\mathrm{d}u\,\mathrm{d}\mathfrak{r} + \mathfrak{r}^2 h_{\alpha\beta}(\mathrm{d}\phi^\alpha + \mathcal{C}^\alpha \mathrm{d}u)(\mathrm{d}\phi^\beta + \mathcal{C}^\beta \mathrm{d}u), \tag{3.1}$$

with $\det h_{\alpha\beta} = \det \omega_{\alpha\beta}$ where $\omega_{\alpha\beta}$ is the unit metric on the $D-2$ sphere. For an asymptotically flat spacetime $h_{\alpha\beta}$ can be expanded as [94]

$$h_{\alpha\beta} = \omega_{\alpha\beta}(\phi^\gamma) + \sum_{s\geqslant 0} \frac{h^{(s+1)}_{\alpha\beta}(u, \phi^\gamma)}{\mathfrak{r}^{D/2+s-1}}, \tag{3.2}$$

and the Bondi news function is obtained from this expansion as the leading-order correction $h^{(1)}_{\alpha\beta}$.

In analogy with the $D = 4$ case, a null frame of vectors is constructed which is asymptotically given by[4]

$$l = -\frac{\partial}{\partial \mathfrak{r}}, \quad k = \frac{\partial}{\partial u} - \frac{1}{2}\frac{\partial}{\partial \mathfrak{r}}, \quad m_{(\alpha)} = \frac{\partial}{\partial \phi^\alpha}. \tag{3.3}$$

Note that all the tetrad vectors are real in contrast to the $D = 4$ dimensional case where the two vectors $m_{(2)}$ and $m_{(3)}$ are often written as two complex null vectors. Next, the components of the Weyl tensor are projected onto the frame (3.3) and the leading order term in the radial coordinate is extracted. Following [1], we denote this quantity by Ω' and its components are given by

$$\Omega'_{(\alpha)(\beta)} \equiv C_{ABCD} k^A m^B_{(\alpha)} k^C m^D_{(\beta)} = -\frac{1}{2}\frac{\hat{e}^\mu_{(\alpha)}\hat{e}^\nu_{(\beta)}\dot{h}^{(1)}_{\mu\nu}}{\mathfrak{r}^{D/2-1}} + \mathcal{O}(\mathfrak{r}^{-D/2}). \tag{3.4}$$

Here $\hat{e}^\beta_{(\alpha)}$ denote a set of vectors forming an orthonormal basis for the unit metric $\omega_{\alpha\beta}$ on the $D-2$ sphere. In practice, this basis is constructed using Gram–Schmidt orthonormalisation starting with the radial unit vector.

As with the Newman–Penrose scalar Ψ_4 in the four dimensional case, we note that this is the contraction of the Weyl tensor with the ingoing null vector twice and two spatial vectors. Whereas in $D = 4$ the two polarisations of the gravitational waves are encoded in the real and

[4] The construction of the exact analogue of the Kinnersley [95] tetrad in general spacetimes at finite radius is subject of ongoing research even in $D = 4$ (see e.g. [34, 96]). In practice, the error arising from the use of an asymptotic form of the tetrad at finite extraction radii is mitigated by extracting at various radii and extrapolating to infinity [37] and we pursue this approach, too, in this work.

imaginary parts of Ψ_4, here $\Omega'_{(\alpha)(\beta)}$ is purely real, with the α, β labels providing the different polarisations.

The final ingredient for extracting the energy radiated in GWs is the rate of change of the Bondi mass given by [94]

$$\dot{M}(u) = \frac{1}{32\pi} \int_{S^{D-2}} \dot{h}^{(1)}_{\alpha\beta} \dot{h}^{(1)\alpha\beta} \mathrm{d}\omega. \tag{3.5}$$

By substituting in for $\dot{h}^{(1)}_{\alpha\beta}$ from the definition of $\Omega'_{(\alpha)(\beta)}$ we obtain an expression for the mass loss.

$$\dot{M}(u) = -\lim_{\mathfrak{r}\to\infty} \frac{\mathfrak{r}^{D-2}}{8\pi} \int_{S^{D-2}} \left(\int_{-\infty}^{u} \Omega'_{(\alpha)(\beta)}(\tilde{u}, \mathfrak{r}, \phi^\gamma) \mathrm{d}\tilde{u} \right)^2 \mathrm{d}\omega, \tag{3.6}$$

where the notation $(\ldots)^2$ implies summation over the (α), (β) labels inside the parentheses, and $\mathrm{d}\omega$ denotes the area element of the $D-2$ sphere. In practice, we will apply equation (3.6) at constant radius $\mathfrak{r}$, therefore replace retarded time u with 'normal' time t and start the integration at $t = 0$ rather than $-\infty$, assuming that GWs generated prior to the start of the simulation can be neglected.

4. Modified cartoon implementation

The formalism summarised in the previous section is valid in generic D dimensional spacetimes with or without symmetries. We now assume that the spacetime under consideration obeys $SO(D-d)$ isometry with $1 \leqslant d \leqslant D-3$, and will derive the expressions required for applying the GW extraction formalism of section 3 to numerical simulations employing the modified Cartoon method.

Throughout this derivation, we will make use of the expressions for scalars, vectors and tensors in spacetimes with $SO(D-d)$ symmetry and the regularisation of their components at $z = 0$ as listed in appendices A and B of [83]. The key result of these relations for our purposes is that the ADM variables α, β^I, γ_{IJ}, K_{IJ} for a spacetime with $SO(D-d)$ isometry can be expressed completely in terms of their d dimensional components β^i, γ_{ij} and K_{ij} as well as two additional functions γ_{ww} and K_{ww} according to

$$\begin{aligned} \beta^I &= (\beta^i, 0), \\ \gamma_{IJ} &= \begin{pmatrix} \gamma_{ij} & 0 \\ 0 & \delta_{ab}\gamma_{ww} \end{pmatrix}, \\ K_{IJ} &= \begin{pmatrix} K_{ij} & 0 \\ 0 & \delta_{ab}K_{ww} \end{pmatrix}, \end{aligned} \tag{4.1}$$

while the scalar α remains unchanged.

From the viewpoint of numerical applications, the key relations of the procedure reviewed in section 3 are equations (3.4) and (3.6). The first provides $\Omega'_{(\alpha)(\beta)}$ in terms of the Weyl tensor and the normal frame, and the second tells us how to calculate the mass loss from $\Omega'_{(\alpha)(\beta)}$. The latter is a straightforward integration conveniently applied as a post processing operation, so that we can focus here on the former equation. For this purpose, we first note that in practice wave extraction is performed in the wave zone far away from the sources. Even if the sources are made up of non-trivial energy matter fields, the GW signal is calculated in vacuum where the Weyl and Riemann tensors are the same. Our task at hand is then twofold: (i) calculate the

Riemann tensor from the ADM variables and (ii) to construct a null frame. These two tasks are the subject of the remainder of this section.

4.1. The Riemann tensor

4.1.1. The (D − 1) + 1 splitting of the Riemann tensor. The ADM formalism is based on a space-time decomposition of the D dimensional spacetime manifold into a one-parameter family of spacelike hypersurfaces which are characterised by a future-pointing, unit normal timelike field n^A. This normal field together with the projection operator

$$\perp^A{}_B = \delta^A{}_B + n^A n_B, \tag{4.2}$$

allows us to split tensor fields into components tangential or orthogonal to the spatial hypersurfaces by contracting each tensor index either with n_A or with $\perp^B{}_A$. For a symmetric rank (0,2) tensor, for example, we thus obtain the following three contributions

$$T_{00} \equiv T_{AB} n^A n^B, \quad \perp T_{0A} = \perp T_{A0} \equiv \perp^C{}_A T_{CB} n^B, \quad \perp T_{AB} \equiv \perp^C{}_A \perp^D{}_B T_{CD}. \tag{4.3}$$

The most important projections for our study are those of the Riemann tensor which are given by the Gauss–Codazzi relations used in the standard ADM splitting of the Einstein equations (see e.g. [87])

$$\perp R_{ABCD} = \mathcal{R}_{ABCD} + K_{AC} K_{BD} - K_{AD} K_{CB}, \tag{4.4}$$

$$\perp R_{A0CD} \equiv \perp (R_{ABCD} n^B) = -D_C K_{AD} + D_D K_{AC}, \tag{4.5}$$

$$\begin{aligned} \perp R_{A0C0} \equiv \perp (R_{ABCD} n^B n^D) &= \perp R_{AC} + \mathcal{R}_{AC} + K K_{AC} - K_{AE} K^E{}_C \\ &= \mathcal{R}_{AC} + K K_{AC} - K_{AE} K^E{}_C, \end{aligned} \tag{4.6}$$

where in the last line we used the fact that in vacuum R_{AC} and, hence, its projection vanishes (note, however, that in general $\mathcal{R}_{AC} \neq 0$ even in vacuum). Furthermore $D_C K_{AD} = \partial_C K_{AD} - \Gamma^B_{CA} K_{BD} - \Gamma^B_{CD} K_{AB}$ is the covariant derivative of the extrinsic curvature defined on the spatial hypersurface, with Christoffel symbols calculated from the induced metric γ_{AB}. Equations (4.4)–(4.6) tell us how to reconstruct the full D dimensional Riemann tensor from $D - 1$ dimensional quantities defined on the spatial hypersurfaces which foliate our spacetime.

From this point on, we will use coordinates adapted to the $(D - 1) + 1$ split. In such coordinates, we can replace in equations (4.4)–(4.6) the spacetime indices A, B, … on the left and right-hand side by spatial indices I, J, … while the time components of the spacetime Riemann tensor are taken into account through the contractions with the unit timelike normal n^A and which we denote with the suffix 0 in (4.5) and (4.6). Note that more than two contractions of the Riemann tensor with the timelike unit normal n^A vanish by symmetry of the Riemann tensor.

4.1.2. The Riemann tensor in SO(D − 3) symmetry. The expressions given in the previous section for the components of the Riemann tensor are valid for general spacetimes with or without symmetries. In this section, we will work out the form of the components of the Riemann tensor in spacetimes with $SO(D - d)$ isometry for $1 \leqslant d \leqslant D - 3$.

For this purpose we recall the Cartesian coordinate system $X^I = (x^{\hat{i}}, z, w^a)$ of equation (2.5), adapted to a spacetime that is symmetric under rotations in any plane spanned by two of the (z, w^a). We discuss in turn how the terms appearing on the right-hand sides of

equations (4.4)–(4.6) simplify under this symmetry. We begin with the components of the spatial Riemann tensor, given in terms of the spatial metric and Christoffel symbols by

$$\mathcal{R}_{IJKL} = \frac{1}{2}(\partial_L\partial_I\gamma_{JK} + \partial_K\partial_J\gamma_{IL} - \partial_K\partial_I\gamma_{JL} - \partial_L\partial_J\gamma_{IK}) \\ -\gamma_{MN}\Gamma^N_{IK}\Gamma^M_{JL} + \gamma_{MN}\Gamma^N_{IL}\Gamma^M_{JK}. \tag{4.7}$$

The rotational symmetry imposes conditions on the derivatives of the metric, the Christoffel symbols and the components of the Riemann tensor that are obtained in complete analogy to the derivation in section 2.2 and appendix A of [83]. We thus calculate all components of the Riemann tensor, where its indices can vary over the coordinates inside and outside the computational domain, and obtain

$$\mathcal{R}_{ijkl} = \frac{1}{2}(\partial_l\partial_i\gamma_{jk} + \partial_k\partial_j\gamma_{il} - \partial_k\partial_i\gamma_{jl} - \partial_l\partial_j\gamma_{ik}) - \gamma_{mn}\Gamma^n_{ik}\Gamma^m_{jl} + \gamma_{mn}\Gamma^n_{il}\Gamma^m_{jk}, \tag{4.8}$$

$$\mathcal{R}_{ajkl} = 0, \tag{4.9}$$

$$\mathcal{R}_{iajb} = \delta_{ab}\mathcal{R}_{iwjw}, \tag{4.10}$$

$$\mathcal{R}_{iwjw} \equiv \frac{\partial_{(i}\gamma_{j)z} - \delta_{z(j}\partial_{i)}\gamma_{ww}}{z} - \delta_{z(i}\frac{\gamma_{j)z} - \delta_{j)z}\gamma_{ww}}{z^2} - \frac{1}{2}\partial_j\partial_i\gamma_{ww} - \gamma_{mn}\Gamma^n_{ij}\Gamma^m_{ww} \\ -\frac{1}{2}\frac{\partial_z\gamma_{ij}}{z} + \frac{\delta_{z(i}\gamma_{j)z} - \delta_{iz}\delta_{jz}\gamma_{ww}}{z^2} + \frac{1}{4}\gamma^{ww}\partial_i\gamma_{ww}\partial_j\gamma_{ww}, \tag{4.11}$$

$$\Gamma^m_{ww} \equiv -\frac{1}{2}\gamma^{ml}\partial_l\gamma_{ww} + \frac{\delta^m_z - \gamma^{mz}\gamma_{ww}}{z}, \tag{4.12}$$

$$\mathcal{R}_{abcl} = 0, \tag{4.13}$$

$$\mathcal{R}_{abcd} = (\delta_{ac}\delta_{bd} - \delta_{bc}\delta_{ad})\mathcal{R}_{wuwu}, \tag{4.14}$$

$$\mathcal{R}_{wuwu} \equiv -\frac{1}{4}\gamma^{mn}\partial_m\gamma_{ww}\partial_n\gamma_{ww} - \gamma_{ww}\frac{\gamma^{zm}}{z}\partial_m\gamma_{ww} + \frac{\gamma_{ww} - \gamma^{zz}\gamma^2_{ww}}{z^2}. \tag{4.15}$$

For the right-hand side of equation (4.6), we also need the spatial Ricci tensor which is obtained from contraction of the Riemann tensor over the first and third index. In $SO(D-d)$ symmetry, its non-vanishing components are

$$\mathcal{R}_{ij} = \gamma^{mn}\mathcal{R}_{minj} + (D-d-1)\gamma^{ww}\mathcal{R}_{iwjw}, \tag{4.16}$$

$$\mathcal{R}_{ab} = \delta_{ab}\mathcal{R}_{ww}, \tag{4.17}$$

$$\mathcal{R}_{ww} \equiv \gamma^{mn}\mathcal{R}_{mwnw} + (D-d-2)\gamma^{ww}\mathcal{R}_{wuwu}. \tag{4.18}$$

Note that the last expression, $\gamma^{ww}\mathcal{R}_{wuwu}$, does *not* involve a summation over w, but merely stands for the product of γ^{ww} with the expression (4.15).

The components of the extrinsic curvature are given by equation (4.1). Its derivative is directly obtained from the expressions (A.1)–(A.12) in appendix A of [83] and can be written as

$$D_i K_{jk} = \partial_i K_{jk} - \Gamma^l_{ij} K_{kl} - \Gamma^l_{ik} K_{lj}, \tag{4.19}$$

$$D_i K_{ab} = \delta_{ab}(\partial_i K_{ww} - K_{ww}\gamma^{ww}\partial_i \gamma_{ww}), \tag{4.20}$$

$$D_a K_{bj} = \delta_{ab}\left(\frac{K_{jz} - \delta_{jz}K_{ww}}{z} - \frac{1}{2}K_{ww}\gamma^{ww}\partial_j\gamma_{ww} - K_{ij}\Gamma^i_{ww}\right). \tag{4.21}$$

Next, we plug the expressions assembled in equations (4.7)–(4.21) into the Gauss–Codazzi equations (4.4)–(4.6) where, we recall, early Latin indices A, B, … are now replaced by I, J, … following our switch to adapted coordinates. Splitting the index range I into (i, a) for components inside and outside the computational domain, and recalling that an index 0 denotes contraction with $\boldsymbol{n}$, we can write the resulting components of the spacetime Riemann tensor as

$$R_{ijkl} = \mathcal{R}_{ijkl} + K_{ik}K_{jl} - K_{il}K_{jk}, \tag{4.22}$$

$$R_{ibkd} = \delta_{bd}R_{iwkw}, \tag{4.23}$$

$$R_{iwkw} \equiv \mathcal{R}_{iwkw} + K_{ik}K_{ww}, \tag{4.24}$$

$$R_{abcd} = (\delta_{ac}\delta_{bd} - \delta_{bc}\delta_{ad})(\mathcal{R}_{wuwu} + K^2_{ww}), \tag{4.25}$$

$$R_{ajkl} = R_{abcl} = 0, \tag{4.26}$$

$$R_{i0kl} = D_l K_{ik} - D_k K_{il}, \tag{4.27}$$

$$R_{a0ck} = \delta_{ac}R_{w0wk}, \tag{4.28}$$

$$R_{w0wk} \equiv \partial_k K_{ww} - \frac{1}{2}\gamma^{ww}K_{ww}\partial_k\gamma_{ww} - \frac{K_{kz} - \delta_{kz}K_{ww}}{z} + \Gamma^m_{ww}K_{mk}, \tag{4.29}$$

$$R_{a0cd} = R_{i0kd} = R_{a0kl} = 0, \tag{4.30}$$

$$R_{i0j0} = \mathcal{R}_{ij} + KK_{ij} - K_{im}K^m_j, \tag{4.31}$$

$$K = \gamma^{mn}K_{mn} + (D - d - 1)\gamma^{ww}K_{ww}, \tag{4.32}$$

$$R_{a0b0} = \delta_{ab}R_{w0w0}, \tag{4.33}$$

$$R_{w0w0} \equiv \mathcal{R}_{ww} + (K - \gamma^{ww}K_{ww})K_{ww}, \tag{4.34}$$

$$R_{a0i0} = 0. \tag{4.35}$$

With these expressions, we are able to calculate all components of the spacetime Riemann tensor directly from the ADM variables γ_{ij}, γ_{ww}, K_{ij} and K_{ww} and their spatial derivatives. There

remains, however, one subtlety arising from the presence of terms containing explicit division by z. Numerical codes employing vertex centered grids need to evaluate these terms at $z = 0$. As described in detail in appendix A, all the above terms involving division by z are indeed regular and can be rewritten in a form where this is manifest with no divisions by zero.

4.2. The null frame

The null frame we need for the projections of the Weyl tensor consists of D unit vectors as given in equation (3.3): (i) the ingoing null vector k^A, (ii) the outgoing null vector l^A which, however, does not explicitly appear in the scalars (3.4) for the outgoing gravitational radiation, and (iii) the $(D-2)$ vectors $m^A_{(\alpha)}$ pointing in the angular directions on the sphere.

We begin this construction with the $D-2$ unit basis vectors on the $D-2$ sphere, $m^A_{(\alpha)}$, and recall for this purpose equation (2.8) that relates our spherical coordinates (r, ϕ^α) to the Cartesian $(\hat{x^i}, z, w^a)$. The set of spatial vectors, although not yet in orthonormalised form, then consists of a radial vector denoted by $\tilde{m}_{(1)}$ and $D-2$ angular vectors $\tilde{m}_{(\alpha)}$ whose components in Cartesian coordinates $X^I = (\hat{x^i}, z, w^a)$ on the computational domain $w^a = 0$ are obtained through the chain rule

$$\tilde{m}_{(1)} = \frac{\partial}{\partial r} = \frac{\partial X^I}{\partial r}\frac{\partial}{\partial X^I} \quad \Rightarrow \quad \tilde{m}^I_{(1)} = \frac{1}{r}(x^1, \ldots, x^{d-1}, z, 0, \ldots, 0), \tag{4.36}$$

$$\tilde{m}_{(\alpha)} = \frac{\partial}{\partial \phi^\alpha} = \frac{\partial X^I}{\partial \phi^\alpha}\frac{\partial}{\partial X^I}. \tag{4.37}$$

We can ignore time components here, because our coordinates are adapted to the spacetime split, so that all spatial vectors have vanishing time components and this feature is preserved under the eventual Gram–Schmidt orthonormalisation. Plugging equation (2.8) into (4.37), we obtain for $\tilde{m}_{(\alpha)}$ (after rescaling by $r \times \sin\phi^2 \times \ldots \times \sin\phi^\alpha$)

$$\underbrace{\begin{pmatrix} -\sum_{s=2}^{D-1}(w^s)^2 \\ w^1 w^2 \\ \vdots \\ \vdots \\ \vdots \\ w^1 w^{D-1} \end{pmatrix}}_{=\tilde{m}^I_{(2)}}, \ldots, \underbrace{\begin{pmatrix} 0 \\ \vdots \\ 0 \end{pmatrix}\}(\alpha-2)\times \\ \begin{pmatrix} -\sum_{s=\alpha}^{D-1}(w^s)^2 \\ w^{\alpha-1}w^\alpha \\ \vdots \\ w^{\alpha-1}w^{D-2} \\ w^{\alpha-1}w^{D-1} \end{pmatrix}}_{=\tilde{m}^I_{(\alpha)}}, \ldots, \underbrace{\begin{pmatrix} 0 \\ \vdots \\ \vdots \\ \vdots \\ 0 \\ -(w^{D-2})^2 - (w^{D-1})^2 \\ w^{D-3}w^{D-2} \\ w^{D-3}w^{D-1} \end{pmatrix}}_{=\tilde{m}^I_{(D-2)}}, \underbrace{\begin{pmatrix} 0 \\ \vdots \\ \vdots \\ \vdots \\ 0 \\ 0 \\ -(w^{D-1})^2 \\ w^{D-2}w^{D-1} \end{pmatrix}}_{=\tilde{m}^I_{(D-1)}}. \tag{4.38}$$

In $D = 4$ dimensions, these vectors, together with $\tilde{m}_{(1)}$ of equation (4.36) would form the starting point for Gram–Schmidt orthonormalisation; see e.g. appendix C in [57]. In $D \geqslant 5$ dimensional spacetimes with $SO(D-d)$ symmetry, however, we face an additional difficulty: on the computational domain $w^a = 0$, all components of the vectors $\tilde{m}_{(d+1)}, \ldots, \tilde{m}_{(D-1)}$ vanish and their normalisation would result in divisions of zero by zero. This difficulty is overcome by rewriting the Cartesian components of the vectors in terms of spherical coordinates and then exploiting the freedom we have in suitably orienting the frame. The details of this procedure are given in appendix B where we derive a manifestly regular set of spatial vectors given by

$$\tilde{m}^A_{(1)} = (0 \mid x^1,\ \ldots,\ x^d \mid 0, \ldots,\ 0), \tag{4.39}$$

$$\tilde{m}^A_{(2)} = (0 \mid -\rho_2^2,\ x^1x^2,\ x^1x^3,\ \ldots,\ x^1x^d \mid 0,\ \ldots,\ 0), \tag{4.40}$$

$$\ldots \quad \ldots$$

$$\tilde{m}^A_{(\hat{\alpha})} = (0, \mid \underbrace{0,\ \ldots,\ 0}_{(\hat{\alpha}-2)\times},\ -\rho^2_{\hat{\alpha}},\ x^{\hat{\alpha}-1}x^{\hat{\alpha}},\ \ldots,\ x^{\hat{\alpha}-1}x^d \mid 0,\ \ldots,\ 0), \tag{4.41}$$

$$\ldots \quad \ldots$$

$$\tilde{m}^A_{(d)} = (0, \mid \underbrace{0,\ \ldots,\ 0}_{(d-2)\times},\ -x^d,\ x^{d-1} \mid 0,\ \ldots,\ 0), \tag{4.42}$$

$$\tilde{m}^A_{(d+1)} = (0 \mid \underbrace{0,\ \ldots,\ 0}_{d\times} \mid 1,\ 0,\ \ldots,\ 0), \tag{4.43}$$

$$\ldots \qquad \ldots$$

$$\tilde{m}^A_{(D-1)} = (0 \mid \underbrace{0,\ \ldots,\ 0}_{d\times} \mid 0,\ \ldots,\ 0,\ 1), \tag{4.44}$$

where $\rho_I = \sum_{s=I}^{D-1}(w^s)^2$, we have restored, for completeness, the time component and the vertical bars highlight the three component sectors: time, spatial on-domain, and spatial off-domain. Equations (4.43) and (4.44) can, of course, be conveniently written in short-hand notation as $\tilde{m}^A_{(a)} = \delta^A{}_a$. For the special case $d = 3$, the vectors are given by

$$\tilde{m}^A_{(1)} = (0 \mid x,\ y,\ z \mid 0, \ldots,\ 0), \tag{4.45}$$

$$\tilde{m}^A_{(2)} = (0 \mid -y^2 - z^2,\ xy,\ xz \mid 0, \ldots,\ 0), \tag{4.46}$$

$$\tilde{m}^A_{(3)} = (0 \mid 0,\ -z,\ y \mid 0,\ \ldots,\ 0), \tag{4.47}$$

$$\tilde{m}^A_{(4)} = (0 \mid 0,\ 0,\ 0 \mid 1,\ 0,\ \ldots,\ 0), \tag{4.48}$$

$$\ldots\ldots \tag{4.49}$$

$$\tilde{m}^A_{(D-1)} = (0 \mid 0,\ 0,\ 0 \mid 0,\ \ldots,\ 0,\ 1), \tag{4.50}$$

The next step is to orthonormalise these vectors. Clearly the vectors $m^A_{(a)}$ with components in the w^a dimensions are normalised by:

$$m^A_{(a)} = \frac{1}{\sqrt{\gamma_{ww}}}\delta^A{}_a \tag{4.51}$$

For the remaining d vectors given by equations (4.39)–(4.42) or, for $d = 3$, the spatial triad consisting of the three vectors (4.45)–(4.47), we use standard Gram–Schmidt orthonormalisation. Note that under this procedure the components outside the computational domain of these vectors remain zero and can therefore be ignored.

The final element of the null frame we need is the ingoing null vector, which we call k^A. Given in [1] as $\partial/\partial u - \frac{1}{2}\partial/\partial\mathfrak{r}$ asymptotically, we transform out of Bondi coordinates, sending

$(u, \mathfrak{r}) \to (t, r)$ and furthermore use the freedom of rescaling this null vector by applying a constant factor of[5] $\sqrt{2}$

$$k^A = \frac{1}{\sqrt{2}}(n^A - m^A_{(1)}) \tag{4.52}$$

Expressing the timelike unit normal field n^A in terms of our gauge variables α, β^I we find

$$k^A = \frac{1}{\sqrt{2}}\left(\frac{1}{\alpha}, -\frac{\beta^I}{\alpha} - m^I_{(1)}\right), \tag{4.53}$$

where $\beta^I = (\beta^i, 0, \ldots, 0)$, $m^I_{(1)} = (m^i_{(1)}, 0, \ldots, 0)$. This result provides the ingoing null vector for any choice of d and is the version implemented in the code.

4.3. The projections of the Weyl tensor

Finally, we calculate the projections of the Weyl tensor that encode the outgoing gravitational radiation

$$\Omega'_{(\alpha)(\beta)} = R_{ABCD} k^A m^B_{(\alpha)} k^C m^D_{(\beta)}, \tag{4.54}$$

(see equation (3.4)) where k^A is given by equation (4.53) and the normal frame vectors $m_{(2)}, \ldots, m_{(D-1)}$ are those obtained from Gram–Schmidt orthonormalising the right-hand sides of equations (4.39)–(4.44).

We first note that $\Omega'_{(\alpha)(\beta)}$ is symmetric in $\alpha \leftrightarrow \beta$, so contractions solely with $m_{(2)}, \ldots, m_{(d)}$ will result in $d(d-1)/2$ components $\Omega'_{(\hat{\alpha})(\hat{\beta})}$. For the special case $d = 3$, we obtain the three components $\Omega'_{(2)(2)}$, $\Omega'_{(2)(3)}$, $\Omega'_{(3)(3)}$. The null vector k has vanishing w components and from equations (4.22)–(4.35) we see that all components of the Riemann tensor where an odd number of indices is in the range $a, b, \ldots$ are zero. The only non-vanishing terms involving the Riemann tensor with off-domain indices $a, b, \ldots$, therefore, have either four such indices or two and contain a Kronecker delta δ_{ab}; see equations (4.23), (4.25), (4.28) and (4.33). As a consequence, the mixed components $\Omega'_{(\hat{\alpha})(a)} = 0$ and the purely off-domain components $\Omega'_{(a)(b)} \propto \delta_{ab}$. The list of all non-vanishing components $\Omega'_{(\alpha)(\beta)}$ is then given by

$$\Omega'_{(\hat{\alpha})(\hat{\beta})} = \frac{1}{4}\Big[R_{0k0l} m^k_{(\hat{\alpha})} m^l_{(\hat{\beta})} - R_{mk0l} m^m_{(1)} m^k_{(\hat{\alpha})} m^l_{(\hat{\beta})} - R_{0kml} m^k_{(\hat{\alpha})} m^m_{(1)} m^l_{(\hat{\beta})} + R_{mknl} m^m_{(1)} m^k_{(\hat{\alpha})} m^n_{(1)} m^l_{(\hat{\beta})}\Big], \tag{4.55}$$

$$\Omega'_{(a)(b)} = \delta_{ab}\, \Omega'_{(w)(w)}\,, \tag{4.56}$$

$$\Omega'_{(w)(w)} = \frac{1}{4\gamma_{ww}}\Big[R_{w0w0} - R_{w0wk} m^k_{(1)} - R_{w0wl} m^l_{(1)} + R_{wkwl} m^k_{(1)} m^l_{(1)}\Big], \tag{4.57}$$

where $\hat{\alpha}, \hat{\beta} = 2, \ldots, d$ and all components of the Riemann tensor on the right-hand sides are listed in the set of equations (4.22)–(4.35). In particular, the components R_{w0w0}, R_{w0wk} and R_{wkwl}, which contain indices in the off-domain directions, are obtained from equations (4.34), (4.29) and (4.24), respectively and thus derived directly from quantities computed in the simulation (the γ_{ij}, K_{ij}, γ_{ww} and K_{ww} that appear on the right-hand sides of these equations or

[5] The convention we adopt here is more common (though not unanimous) in numerical relativity.

enter in the calculation of the spatial Riemann tensor). It should be noted here that $\Omega'_{(\alpha)(\beta)}$ is trace free, and so $\Omega'_{(w)(w)}$ can be calculated from the diagonal terms $\Omega'_{(2)(2)}, \ldots \Omega'_{(d)(d)}$. In a numerical simulation, the components of $\Omega'_{(\alpha)(\beta)}$ are calculated as functions of time and then can be integrated according to equation (3.6) to extract the amount of energy radiated in gravitational waves.

4.4. SO(2) symmetry

In the axisymmetric case $d = D - 2$ there exists only one w direction (off domain). As discussed in section 4 of [83], we keep all tensor components as we would in the absence of symmetry, and the modified Cartoon method and, thus, the rotational symmetry only enters in the calculation of spatial derivatives in the w direction. For $SO(2)$ symmetry, the extraction of gravitational waves therefore proceeds as follows.

- All components of the ADM metric and extrinsic curvature are extracted on the $D - 2$ dimensional computational domain.
- The spatial Riemann tensor and its contractions are directly evaluated using equation (4.7) with the relations of appendix C in [83] for off-domain derivatives.
- The necessary components of the spacetime Riemann tensor and its projections onto the timelike unit normal are evaluated through equations (4.4)–(4.6).
- The null frame is constructed as detailed in section 4.2, simply setting $d = D - 2$.
- All the projections of the Weyl tensor onto the null frame vectors are obtained from equation (4.55), but now covering the entire range of spatial indices

$$\Omega'_{(\alpha)(\beta)} = \frac{1}{4}\Big[R_{0K0L}m^K_{(\alpha)}m^L_{(\beta)} - R_{MK0L}m^M_{(1)}m^K_{(\alpha)}m^L_{(\beta)} - R_{0KML}m^K_{(\alpha)}m^M_{(1)}m^L_{(\beta)} + R_{MKNL}m^M_{(1)}m^K_{(\alpha)}m^N_{(1)}m^L_{(\beta)}\Big]. \tag{4.58}$$

Note that with the existence of more components of the Riemann tensor, more projections of the Weyl tensor now exist, specifically cross-terms such as $\Omega'_{(2)(w)}$. This can be seen straightforwardly by using $SO(2)$ modified Cartoon terms from appendix C of [83] and the expressions for the full and spatial Riemann tensor given in equations (4.4) and (4.7). For example, we can see that a component such as R_{wijk} is non-zero. This will contribute to terms of the form $\Omega'_{(\hat{\alpha})(w)}$. As already emphasised in [83], the key gain in employing the modified Cartoon method for simulating axisymmetric spacetimes does *not* lie in the elimination of tensor components, but in the dimensional reduction of the computational domain.

5. Numerical simulations

In the remainder of this work, we will implement the specific version of the wave extraction for $d = 3$ and $D = 6$ and simulate head-on collisions of equal-mass, non-spinning BHs starting from rest. We will calibrate the numerical uncertainties arising from the numerical discretisation of the equations (fourth order in space and time and second order at the outer and refinement boundaries), the use of large but finite extraction radii and also consider the dependency of the results on the initial separation of the BHs. This type of collisions has already been studied by Witek *et al* [69] who calculate the GW energy using the Kodama–Ishibashi formalism, which enables us to compare our findings with their values.

5.1. Code infrastructure and numerical set-up

We perform evolutions using the LEAN code [57, 97] which is based on CACTUS [98, 99] and uses CARPET [100, 101] for mesh refinement. The Einstein equations are implemented in the BSSN formulation with the modified Cartoon method employed to reduce computational cost. For the explicit equations under the $SO(D-3)$ symmetry that we use, see section 3.2 of [83] with parameter $d = 3$. Without loss of generality, we perform collisions along the x axis, such that the centre-of mass is located at the origin of the grid, and impose octant symmetry.

We specify the gauge in terms of the '1 + log' and 'Γ driver' conditions for the lapse function and shift vector (see e.g. [102]) according to

$$\partial_t \alpha = \beta^m \partial_m \alpha - 2\alpha K, \tag{5.1}$$

$$\partial_t \beta^i = \beta^m \partial_m \beta^i + \frac{1}{4}\tilde{\Gamma}^i - \frac{1}{2^{1/3} R_h}\beta^i, \tag{5.2}$$

with initial values $\alpha = 1$, $\beta^i = 0$.

The BH initial data is calculated using the higher dimensional generalisation of Brill–Lindquist data [103, 104] given in terms of the ADM variables by

$$K_{IJ} = 0, \quad \gamma_{IJ} = \psi^{4/(D-3)}\delta_{IJ}, \quad \psi = 1 + \sum_{\mathcal{N}} \frac{\mu_{\mathcal{N}}}{4\left[\sum_{K=1}^{D-1}(X^K - X^K_{\mathcal{N}})^2\right]^{(D-3)/2}}, \tag{5.3}$$

where the summation over $\mathcal{N}$ and K extends over the multiple BHs and spatial coordinates, respectively, and $X^K_{\mathcal{N}}$ denotes the position of the $\mathcal{N}$th BH. As mentioned above, we place the BHs on the x axis in the centre-of-mass frame, so that in the equal-mass case, we have $X^1_{\mathcal{N}} = \pm x_0$. Our initial configuration is therefore completely specified by the initial separation which we measure in units of the horizon radius R_h of a single BH. The BH mass and the radius R_h are related through the mass parameter μ by

$$\mu = \frac{16\pi M}{(D-2)\mathcal{A}_{D-2}}, \quad \mu = R_{\rm h}^{D-3}, \quad \mathcal{A}_{D-2} = \frac{2\pi^{(D-1)/2}}{\Gamma\left(\frac{D-1}{2}\right)}, \tag{5.4}$$

where $\mathcal{A}_{D-2}$ is the surface area of the unit $(D-2)$ sphere.

The computational domain used for these simulations consists of a set of eight nested refinement levels which we characterise in terms of the following parameters: (i) the resolution h on the innermost level which gets coarser by a factor of two on each consecutive outer level, (ii) the size L of the domain which describes the distance of the outermost edge from the origin, and (iii) the resolution H on the refinement level where the gravitational waves are extracted.

For each simulation, we calculate the $\Omega'_{(\alpha)(\beta)}$ on our three dimensional computational grid and project them onto a two dimensional array representing a spherical grid at fixed coordinate radius. The data thus obtained on the extraction sphere are inserted into equation (3.6). The $\Omega'_{(\alpha)(\beta)}$ are scalars and so in our angular coordinate system do not depend on $\phi^4, \ldots, \phi^{D-1}$, so the integral over the sphere in (3.6) can be simplified:

$$\dot{M}(u) = -\lim_{r\to\infty} \frac{r^{D-2}}{8\pi}\mathcal{A}_{D-4}\int_0^\pi \int_0^\pi I[\Omega'^2]\ \sin^{D-3}(\phi^2)\ \sin^{D-4}(\phi^3)\,{\rm d}\phi^3{\rm d}\phi^2, \tag{5.5}$$

where $I[\Omega'^2] \equiv \left(\int_{-\infty}^{u} \Omega'_{(\alpha)(\beta)}\,{\rm d}\tilde{u}\right)^2$. A final integration over time of the variable $\dot{M}$ then gives the total radiated energy.

5.2. Numerical results

We begin our numerical study with an estimate of the uncertainty in our GW estimates arising from the discretisation of the equations. For this purpose, we have evolved two BHs initially located at at $x = \pm x_0 = \pm 4.0\, R_h$ using a computational grid of size $L = 181 R_h$ and three resolutions $h_1 = R_h/50.8$, $h_2 = R_h/63.5$ and $h_3 = R_h/76.2$ which corresponds to $H_1 = R_h/2.12$, $H_2 = R_h/2.65$ and $H_3 = R_h/3.17$ in the extraction zone.

We measure the radiated energy in units of the total ADM mass of the spacetime, which for Brill–Lindquist data is given by equation (5.4) with $\mu \equiv \mu_1 + \mu_2$, the mass parameters of the initial BHs. The radiated energy as a function of time is shown in the upper panel of figure 2. The radiation is almost exclusively concentrated within a window of $\Delta t \approx 20\, R_h$ around merger. During the infall and the post-merger period, in contrast, $E_{\rm rad}$ remains nearly constant. In comparison with collisions in $D = 4$ dimensions, we find the burst of spurious (colloquially referred to as 'junk') radiation significantly weaker, presumably because the Brill–Lindquist data in higher D more closely represent two black holes in isolation due to the higher fall-off rate of the gravitational interaction. By comparing the high-resolution result with that obtained for the coarser grids, we can test the order of convergence. To leading order, the numerical result f_h for some variable obtained at finite resolution h is related to the continuum limit solution f by $f = f_h + \mathcal{O}(h^n)$, where n denotes the order of convergence. By evaluating the quotient

$$Q_n = \frac{f_{h_1} - f_{h_2}}{f_{h_2} - f_{h_3}} = \frac{(h_1/h_2)^n - 1}{1 - (h_3/h_2)^n}, \tag{5.6}$$

we can then plot the two differences $f_{h_1} - f_{h_2}$ and $f_{h_2} - f_{h_3}$ and test whether their ratio is consistent with a given value n. The results for our study are shown in the lower panel of figure 2 which demonstrates that our numerical results converge at fourth order. The discretisation error of the total radiated energy is then obtained as the difference between the finite resolution result and that predicted by Richardson extrapolation (see upper panel in the figure). We obtain for the high-resolution case a total radiated energy $E_{\rm rad} = 8.19 \times 10^{-4}\, M_{\rm ADM}$ with a discretisation error of $\sim 0.4\%$, but note that the error in the cumulative energy peaks at a larger value of a few % during the sharp increase of $E_{\rm rad}(t)$ marking the merger phase.

A second source of error arises from the extraction at finite radius. Following standard practice (see e.g. [37]), we estimate this uncertainty by extracting the GW energy at a set of seven or eight finite radii in the range $40R_h$ to $110R_h$ and extrapolating these values assuming a functional dependency

$$E_{\rm rad}(r) = E_{\rm rad}(\infty) + \frac{a}{r} + \mathcal{O}\left(\frac{1}{r^2}\right), \tag{5.7}$$

where a is a coefficient obtained through the fitting of the numerical data. By applying this procedure, we estimate the uncertainty due to the extraction radius at 0.2% at $R_{\rm ex} = 110\, {\rm R_h}$ and 0.4% at $R_{\rm ex} = 60\, R_h$.

An independent check of our results is available in comparing the radiated energy with the predictions of the perturbative extraction method [66] based on the Kodama–Ishibashi formalism. For this purpose, we have calculated using $h_3 = R_h/76.2$ the gravitational-wave energy radiated in the quadrupole mode as predicted by the Kodama–Ishibashi formalism. Contributions from higher-order multipoles are negligible for this comparison; for odd l they vanish completely by symmetry and for even l up to $l = 8$ they are well below the numerical uncertainty budget. This quadrupole energy is compared with the result obtained from the Weyl tensor in figure 3. The difference for the total radiated energy is about 0.3%, though a larger temporary discrepancy for $E_{\rm rad}$ as a function of time is encountered during the steep

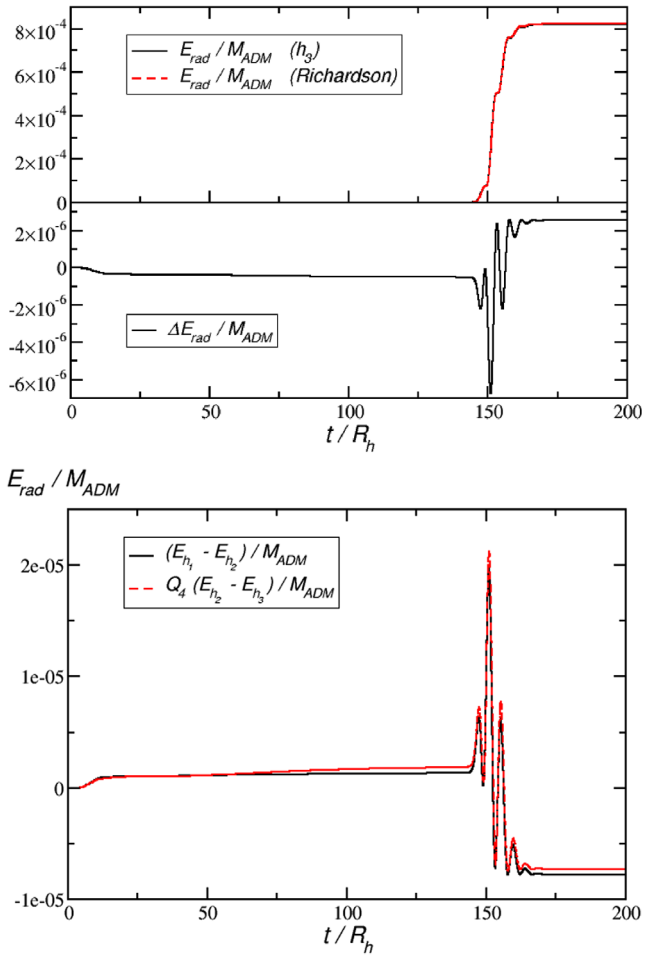

Figure 2. Upper panel: radiated energy as a function of time obtained for the highest resolution $h_3 = R_h/76.2$ (solid curve) and Richardson extrapolated to infinite resolution assuming fourth-order convergence (dashed curve). The curves are nearly on top of each other and we plot in the lower half of the panel their difference to show the level of agreement. Lower panel: convergence plot for the radiated energy $E_{\rm rad}$ extracted at $r_{\rm ex} = 50.4\,R_h$ from an equal-mass collision of two non-spinning BHs in $D = 6$ starting from a separation $8R_h$. The results shown have been obtained using resolutions $h_1 = R_h/50.8$, $h_2 = R_h/63.5$ and $h_3 = R_h/76.2$. The difference in radiated energy between the medium and high-resolution simulations has been rescaled by a factor $Q_4 = 2.784$ expected for fourth-order convergence.

increase at merger, up to a few %. This discrepancy is within the error budget of the two extraction methods.

Finally, we have measured the dependency of the total radiated energy on the initial separation of the BHs. In addition to the simulations discussed so far, we have performed high-resolution simulations placing the BHs at $x_0 = \pm\,7.8\,R_h$ and $x_0 = \pm\,12.8\,R_h$. We have found very small variations at a level of 0.1% in the radiated energy for these cases, well below the combined error budget obtained above. Compared with collisions in $D = 4$ dimensions (see e.g. table II in [57]), $E_{\rm rad}$ shows significantly weaker variation with initial separation in

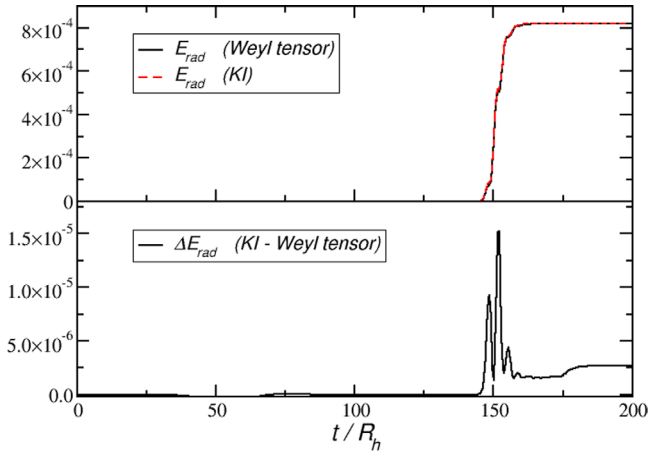

Figure 3. Gravitational wave energy $E_{\rm rad}$ as a function of time using $h_3 = R_h/76.2$ and extracted at $r_{\rm ex} = 50.4\,R_h$ for the $D = 6$ equal-mass head-on collision. The prediction by the new formalism is compared with that of the Kodama–Ishibashi formalism for the quadrupole mode (the higher-order multipoles provide negligible contributions in this case). The bottom panel shows the differences between the two curves.

$D = 6$. We attribute this to the more rapid fall-off of the force of gravity in higher dimensions leading to a prolonged but dynamically slow infall phase which generates barely any GWs.

In summary, we find the total energy radiated in gravitational waves in a head-on collision of two equal-mass, non-spinning BHs to be

$$E_{\rm rad} = (8.19 \pm 0.05) \times 10^{-4}\, M_{\rm ADM}, \tag{5.8}$$

in excellent agreement with the value $(8.1 \pm 0.4) \times 10^{-4}$ reported in the independent study by [69] using dimensional reduction by isometry and the Kodama–Ishibashi formalism.

6. Conclusions

The extraction of gravitational waves from numerical simulations is one of the most important diagnostic tools in studying the strong-field dynamics of compact objects in four as well as higher dimensional spacetimes. In this work we have formulated the Weyl tensor based wave extraction technique of Godazgar and Reall [1]—a higher dimensional generalisation of the Newman–Penrose scalars—in a form suitable for numerical simulations of $D > 4$ dimensional spacetimes with $SO(D-d)$, $1 \leqslant d \leqslant D-2$, symmetry employing the modified Cartoon method. The only prerequisite for implementing our formalism is the availability of the ADM variables on each spatial hypersurface of the effective computational domain. These are constructed straightforwardly from all commonly used numerical evolution systems such as BSSN, generalised harmonic or conformal Z4.

The recipe for extracting the GW signal then consists of the following steps.

(1) Computation of the on and off-domain components of the spatial Riemann tensor (which equals the Weyl tensor in the vacuum extraction region) and the derivative of the extrinsic curvature according to equations (4.8)–(4.21).
(2) Reconstruction of the components of the spacetime Riemann tensor as well as its contractions with the unit timelike normal from the quantities of the previous step according to equations (4.22)–(4.35).

(3) Construction of the null-frame vectors through Gram–Schmidt orthonormalising the expressions of equations (4.39)–(4.44) and then using (4.53) for the ingoing null vector.
(4) Calculation of the projections $\Omega'_{(\alpha)(\beta)}$ of the Weyl tensor onto the null frame vectors using equations (4.55)–(4.57).
(5) Calculation of the energy flux in GWs through equation (3.6) and integration in time of the flux to obtain the total radiated energy.

The most common case of modelling higher dimensional spacetimes with rotational symmetries is the case of $d = 3$ effective spatial dimensions which allows for straightforward generalisation of existing codes (typically developed for $3 + 1$ spacetimes) and also accommodates sufficiently complex dynamics to cover most of the important applications of higher dimensional numerical relativity. We have, for this purpose, explicitly given the specific expressions of some of our relations for $d = 3$ where these are not trivially derived from their general counterparts.

For testing the efficacy and accuracy of this method, we have applied the wave extraction to the study of equal-mass, non-spinning head-on collisions of BHs starting from rest in $D = 6$ using $d = 3$. We find these collisions to radiate a fraction $(8.19 \pm 0.05) \times 10^{-4}$ of the ADM mass in GWs, in excellent agreement with a previous study [69] employing a perturbative extraction technique based on the Kodama–Ishibashi formalism. We find this energy to be essentially independent of the initial separation which we have varied from 8.0 to 15.6 and 25.6 times the horizon radius of a single BH. We attribute this result to the higher fall-off rate of the gravitational attraction in higher dimensions and the correspondingly slow dynamics during the infall stage.

We finally note that the Weyl tensor based wave extraction ideally complements the perturbative extraction technique of the Kodama–Ishibashi formalism. The latter provides the energy contained in individual (l,m) radiation multipoles but inevitably requires cutoff at some finite l. In contrast, the $\Omega'_{(\alpha)(\beta)}$ facilitate calculation of the total radiation, but without multipolar decomposition. It is by putting both extraction techniques together, that we obtain a comprehensive description of the entire wave signal. Future applications include the stability of highly spinning BHs and their transition from unstable to stable configurations, the wave emission in evolutions of black rings and an extended study of higher dimensional BH collisions over a wider range of dimensionality D, initial boosts and with non-zero impact parameter. These studies require particularly high resolution to accurately model the rapid fall-off of gravity, especially for $D \gg 4$, and are therefore beyond the scope of the present study. However, the foundation for analysing in detail the GW energy emission in these and many more scenarios is now available in as convenient a form as in the more traditional $3 + 1$ explorations of numerical relativity.

Acknowledgments

We thank Pau Figueras, Mahdi Godazgar, Markus Kunesch, Harvey Reall, Saran Tunyasuvunakool and Helvi Witek for highly fruitful discussions of this topic. This work has received funding from the European Union's Horizon 2020 research and innovation programme under the Marie SkŁodowska-Curie grant agreement No 690904, from H2020-ERC-2014-CoG Grant No. 'MaGRaTh' 646597, from STFC Consolidator Grant No. ST/L000636/1, the SDSC Comet, PSC-Bridges and TACC Stampede clusters through NSF-XSEDE Award Nos. PHY-090003, the Cambridge High Performance Computing Service Supercomputer Darwin using Strategic Research Infrastructure Funding from the HEFCE and the STFC, and

DiRAC's Cosmos Shared Memory system through BIS Grant No. ST/J005673/1 and STFC Grant Nos. ST/H008586/1, ST/K00333X/1. WGC is supported by a STFC studentship.

Appendix A. Regularisation of terms at $z = 0$

For the axisymmetric case $d = D - 2$, we only need to regularise terms appearing in the calculation of derivatives in the off-domain w direction. All these terms are given explicitly in appendix C of [83], so that in the following we can focus exclusively on the additional terms appearing for $1 \leqslant d \leqslant D - 3$, i.e. for spacetimes admitting two or more rotational Killing vector fields.

The treatment of these terms proceeds in close analogy to that of the BSSN equations in the modified Cartoon approach as described in detail in appendix B of [83]. In contrast to that work, however, we will not be using the conformally rescaled metric of the BSSN equations, which satisfies the simplifying condition $\det \tilde{\gamma} = 1$, and so certain regularised terms involving the inversion of the metric will differ from the expressions obtained for the BSSN equations.

We start with a brief summary of the techniques and the main assumptions we will use to regularise expressions:

A.1. Regularity

We require all tensor components and their derivatives to be regular when expressed in Cartesian coordinates. Under transformation to spherical coordinates this implies that tensors containing an odd (even) number of radial indices, i.e. z indices in our notation, contain exclusively odd (even) powers of z in a series expansion around $z = 0$. Using such a series expansion enables us to trade divisions by z for derivatives with respect to z. For example, for the z component of a vector field $\boldsymbol{V}$, we obtain

$$\frac{V^z}{z} = \frac{a_1 z + a_3 z^3 + \dots}{z} = a_1 + a_3 z^2 + \dots \stackrel{*}{=} a_1 \stackrel{*}{=} \partial_z V^z, \tag{A.1}$$

where we have introduced the symbol $\stackrel{*}{=}$ to denote equality in the limit $z \to 0$.

A.2. Absence of conical singularities

We require that the spacetime contain no conical singularity at the origin $z = 0$. For the implications of this condition, we consider the coordinate transformation from $(x^{\hat{i}}, z, w^{d+1}, \dots, w^a \dots, w^{D-1})$ to $(x^{\hat{i}}, \rho, w^{d+1}, \dots, w^{a-1}, \varphi, w^{a+1}, \dots, w^{D-1})$. As no other w^b, $b \neq a$, coordinates will enter into this discussion we shall refer to w^a as w. In these coordinates we have that

$$\gamma_{\rho\rho} = \frac{z^2}{\rho^2}\gamma_{zz} + 2\frac{zw}{\rho^2}\gamma_{zw} + \frac{w^2}{\rho^2}\gamma_{ww}, \tag{A.2}$$

$$\gamma_{\varphi\varphi} = w^2\gamma_{zz} - 2wz\gamma_{zw} + z^2\gamma_{ww}, \tag{A.3}$$

and the line element for vanishing $\mathrm{d}x^{\hat{i}} = 0$ and $\mathrm{d}w^b = 0$, $b \neq a$, is given by

$$\mathrm{d}s^2 = \gamma_{\rho\rho}\mathrm{d}\rho^2 + \gamma_{\varphi\varphi}\mathrm{d}\varphi^2. \tag{A.4}$$

Requiring the circumference to be the radius times 2π, we have that $\gamma_{\varphi\varphi} = \rho^2\gamma_{\rho\rho}$. Substituting the above expressions and taking the limit $z \to 0$, we obtain

$$\gamma_{zz} - \gamma_{ww} \overset{*}{=} \mathcal{O}(z^2). \tag{A.5}$$

Taking the time derivative of this relation and using the definition of the extrinsic curvature, we find that likewise

$$K_{zz} - K_{ww} \overset{*}{=} \mathcal{O}(z^2). \tag{A.6}$$

A.3. Inverse metric

Various terms that we need to address contain factors of the inverse metric γ^{IJ}. In the practical regularisation procedure, these terms are conveniently handled by expressing γ^{IJ} in terms of the downstairs metric components γ_{ij} and γ_{ww} which are the fields we evolve numerically. We know the metric takes the following form:

$$\gamma_{IJ} = \left(\begin{array}{cccc|cccc} \gamma_{x^1x^1} & \cdots & \gamma_{x^1x^{d-1}} & \gamma_{x^1z} & 0 & 0 & \cdots & 0 \\ \vdots & \ddots & \vdots & \vdots & \vdots & \vdots & \cdots & \vdots \\ \gamma_{x^{d-1}x^1} & \cdots & \gamma_{x^{d-1}x^{d-1}} & \gamma_{x^{d-1}z} & 0 & 0 & \cdots & 0 \\ \gamma_{zx^1} & \cdots & \gamma_{zx^{d-1}} & \gamma_{zz} & 0 & 0 & \cdots & 0 \\ \hline 0 & \cdots & 0 & 0 & \gamma_{ww} & 0 & \ldots & 0 \\ 0 & \cdots & 0 & 0 & 0 & \gamma_{ww} & \ldots & 0 \\ \vdots & \cdots & \vdots & \vdots & \vdots & \vdots & \ddots & \vdots \\ 0 & \cdots & 0 & 0 & 0 & 0 & \cdots & \gamma_{ww} \end{array}\right), \tag{A.7}$$

and we shall denote the upper left quadrant by the matrix M_{ij}. For simplicity, we will use the index $\hat{i}$ to denote $x^{\hat{i}}$ in this section, so e.g. cofactors $C_{12} = C_{x^1x^2}$ and $C_{1z} = C_{x^1z}$. Similarly the indices $i, j, \ldots$ will stand for the x^i, i.e. include the z component.

We can now write the cofactor of an element in the top left quadrant of γ_{IJ} as

$$C_{ij} = (-1)^{i+j}\gamma_{ww}^{\eta}\det(M_{kl\{k\neq j, l\neq i\}}) \tag{A.8}$$

where $\eta = D - d - 1$ and the notation $\det(M_{kl\{k\neq j, l\neq i\}})$ denotes the determinant of the matrix obtained by crossing out the jth row and ith column of M_{kl}. Likewise, we may add further inequalities inside the braces to denote matrices obtained by crossing out more than one row and column. We can then use this expression for C_{ij} and the determinant of the right hand side of equation (A.7),

$$\begin{aligned} \det\gamma_{IJ} &= \gamma_{ww}^{\eta}\det\gamma_{ij} \\ &\overset{*}{=} \gamma_{ww}^{\eta}\gamma_{zz}\det(M_{kl\{k\neq z, l\neq z\}}), \end{aligned} \tag{A.9}$$

in order to obtain expressions for inverse metric components according to

$$\gamma^{ij} = \frac{C_{ij}}{\det\gamma_{IJ}}. \tag{A.10}$$

For $d = 3$, this procedure starts from the spatial metric

$$\gamma_{IJ} = \left(\begin{array}{ccc|ccc} \gamma_{xx} & \gamma_{xy} & \gamma_{xz} & 0 & \cdots & 0 \\ \gamma_{yx} & \gamma_{yy} & \gamma_{yz} & 0 & \cdots & 0 \\ \gamma_{zx} & \gamma_{zy} & \gamma_{zz} & 0 & \cdots & 0 \\ \hline 0 & 0 & 0 & \gamma_{ww} & \ldots & 0 \\ \vdots & \vdots & \vdots & \vdots & \ddots & \vdots \\ 0 & 0 & 0 & 0 & \cdots & \gamma_{ww} \end{array}\right). \tag{A.11}$$

The components C_{ij} of the cofactor matrix (which is symmetric) are given by

$$\begin{array}{lll} C_{xx} = \gamma^{\eta}_{ww}(\gamma_{yy}\gamma_{zz} - \gamma^2_{yz}), & C_{xy} = -\gamma^{\eta}_{ww}(\gamma_{yx}\gamma_{zz} - \gamma_{zx}\gamma_{yz}), & C_{xz} = \gamma^{\eta}_{ww}(\gamma_{yx}\gamma_{zy} - \gamma_{zx}\gamma_{yy}), \\ \cdots & C_{yy} = \gamma^{\eta}_{ww}(\gamma_{xx}\gamma_{zz} - \gamma^2_{zx}), & C_{yz} = -\gamma^{\eta}_{ww}(\gamma_{xx}\gamma_{zy} - \gamma_{zx}\gamma_{xy}), \\ \cdots & \cdots & C_{zz} = \gamma^{\eta}_{ww}(\gamma_{xx}\gamma_{yy} - \gamma^2_{xy}), \end{array} \tag{A.12}$$

the determinant becomes

$$\begin{aligned} \det \gamma_{IJ} &= \gamma^{\eta}_{ww}(\gamma_{xx}\gamma_{yy}\gamma_{zz} + 2\gamma_{xy}\gamma_{xz}\gamma_{yz} - \gamma_{xx}\gamma^2_{yz} - \gamma_{yy}\gamma^2_{xz} - \gamma_{zz}\gamma^2_{xy}) \\ &\overset{*}{=} \gamma^{\eta}_{ww}\gamma_{zz}(\gamma_{xx}\gamma_{yy} - \gamma^2_{xy}), \end{aligned} \tag{A.13}$$

and the inverse metric follows by inserting these into equation (A.10).
Using these techniques, we can regularise all terms in equations (4.11), (4.12), (4.15), (4.21) and (4.29) that contain divisions by z. It turns out to be convenient to combine the individual terms into the following six expressions.

(1)

$$\frac{\delta^i_z - \gamma^{zi}\gamma_{ww}}{z}$$

We express γ^{zi} in terms of the metric, and trade divisions by z for derivatives ∂_z and obtain

$$\frac{\delta^i_z - \gamma^{zi}\gamma_{ww}}{z} \overset{*}{=} \begin{cases} \sum_{\hat{j}=1}^{d-1}(-1)^{\hat{i}+\hat{j}} \dfrac{\gamma_{ww}}{\det M_{mn}} \partial_z \gamma_{z\hat{j}} \det(M_{kl\{k\neq\hat{i},k\neq z,l\neq z,l\neq\hat{j}\}}) & \text{if } i = \hat{i} \\ 0 & \text{if } i = z \end{cases} \tag{A.14}$$

For the $d = 3$ case this reduces to

$$\frac{\delta^i_z - \gamma^{zi}\gamma_{ww}}{z} \overset{*}{=} \begin{cases} \dfrac{\gamma_{yy}\partial_z\gamma_{xz} - \gamma_{xy}\partial_z\gamma_{yz}}{\gamma_{xx}\gamma_{yy} - \gamma^2_{xy}} & \text{if } i = x \\ \dfrac{\gamma_{xx}\partial_z\gamma_{yz} - \gamma_{xy}\partial_z\gamma_{xz}}{\gamma_{xx}\gamma_{yy} - \gamma^2_{xy}} & \text{if } i = y \\ 0 & \text{if } i = z \end{cases}. \tag{A.15}$$

(2)

$$\frac{\partial_i\gamma_{jz}-\delta_{jz}\partial_i\gamma_{ww}}{z}-\delta_{iz}\frac{\gamma_{jz}-\delta_{jz}\gamma_{ww}}{z^2}+\frac{\partial_j\gamma_{iz}-\delta_{iz}\partial_j\gamma_{ww}}{z}-\delta_{jz}\frac{\gamma_{iz}-\delta_{iz}\gamma_{ww}}{z^2}$$

Here we simply trade divisions by z for ∂_z and obtain

$$\begin{aligned}&\frac{\partial_i\gamma_{jz}-\delta_{jz}\partial_i\gamma_{ww}}{z}-\delta_{iz}\frac{\gamma_{jz}-\delta_{jz}\gamma_{ww}}{z^2}+\frac{\partial_j\gamma_{iz}-\delta_{iz}\partial_j\gamma_{ww}}{z}-\delta_{jz}\frac{\gamma_{iz}-\delta_{iz}\gamma_{ww}}{z^2}\\&\stackrel{*}{=}\begin{cases}2\partial_z\partial_{(\hat{i}}\gamma_{\hat{j})z} & \text{if } i=\hat{i},\ j=\hat{j}\\ 0 & \text{if } (i,j)=(\hat{i},z) \text{ or } (z,\hat{j})\\ \partial_z\partial_z(\gamma_{zz}-\gamma_{ww}) & \text{if } i=j=z\end{cases}.\end{aligned}\tag{A.16}$$

(3)

$$-\frac{1}{2}\frac{\partial_z\gamma_{ij}}{z}+\frac{\delta_{z(i}\gamma_{j)z}-\delta_{iz}\delta_{jz}\gamma_{ww}}{z^2}$$

We use $\gamma_{zz}-\gamma_{ww}\stackrel{*}{=}\mathcal{O}(z^2)$ and trade a division by z for a z derivative. The result is

$$-\frac{1}{2}\frac{\partial_z\gamma_{ij}}{z}+\frac{\delta_{z(i}\gamma_{j)z}-\delta_{iz}\delta_{jz}\gamma_{ww}}{z^2}\stackrel{*}{=}\begin{cases}-\frac{1}{2}\partial_z\partial_z\gamma_{\hat{i}\hat{j}} & \text{if } i=\hat{i},\ j=\hat{j}\\ 0 & \text{if } (i,j)=(\hat{i},z) \text{ or } (z,\hat{j})\\ -\frac{1}{2}\partial_z\partial_z\gamma_{ww} & \text{if } i=j=z\end{cases}.\tag{A.17}$$

(4)

$$\frac{\gamma_{ww}\gamma^{zj}\partial_j\gamma_{ww}}{z}$$

Using equations (A.7)–(A.10), we express the inverse metric components γ^{zj} in terms of the downstairs metric and trade the division by z for a z derivative. We thus obtain

$$\begin{aligned}\frac{\gamma_{ww}\gamma^{zj}\partial_j\gamma_{ww}}{z}&\stackrel{*}{=}\sum_{\hat{j}=1}^{d-1}\sum_{\hat{m}=1}^{d-1}(-1)^{\hat{m}+\hat{j}-1}\frac{\gamma_{ww}}{\det(M_{pq})}\partial_{\hat{j}}\gamma_{ww}\partial_z\gamma_{z\hat{m}}\det(M_{kl\{k\neq\hat{j},k\neq z,l\neq z,l\neq\hat{m}\}})\\&\quad+\frac{\gamma_{ww}\det(M_{kl\{k\neq z,l\neq z\}})}{\det(M_{pq})}\partial_z\partial_z\gamma_{ww}.\end{aligned}\tag{A.18}$$

which in the case $d=3$ reduces to

$$\begin{aligned}\frac{\gamma_{ww}\gamma^{zj}\partial_j\gamma_{ww}}{z}&\stackrel{*}{=}\frac{(\gamma_{yx}\partial_z\gamma_{zy}-\gamma_{yy}\partial_z\gamma_{zx})\partial_x\gamma_{ww}+(\gamma_{yx}\partial_z\gamma_{zx}-\gamma_{xx}\partial_z\gamma_{yz})\partial_y\gamma_{ww}}{\gamma_{xx}\gamma_{yy}-\gamma_{xy}^2}\\&\quad+\partial_z\partial_z\gamma_{ww}.\end{aligned}\tag{A.19}$$

(5)

$$\frac{\gamma^{zz}\gamma_{ww}^2-\gamma_{ww}}{z^2}$$

The regularisation of this term proceeds in analogy to that of term (9) in appendix B of [83], except we do not set $\det\gamma = 1$. By rewriting $1 = \gamma^{zz}/\gamma^{zz} = \gamma^{zz}\det\gamma_{IJ}/C_{zz}$, trading divisions by z for z derivatives and using $\gamma_{zz} \overset{*}{=} \gamma_{ww} + \mathcal{O}(z^2)$, we obtain

$$\frac{\gamma^{zz}\gamma_{ww}^2 - \gamma_{ww}}{z^2} \overset{*}{=} \frac{1}{2}\partial_z\partial_z(\gamma_{ww} - \gamma_{zz}) - \frac{\sum_{\hat{i}=1}^{d-1}\sum_{\hat{m}=1}^{d-1}(-1)^{\hat{i}+\hat{m}-1}\partial_z\gamma_{z\hat{i}}\partial_z\gamma_{z\hat{m}}\det(M_{kl\{k\neq\hat{i},k\neq z,l\neq z,l\neq\hat{m}\}})}{\det(M_{kl\{k\neq z,l\neq z\}})}. \tag{A.20}$$

which in the case $d = 3$ reduces to

$$\frac{\gamma^{zz}\gamma_{ww}^2 - \gamma_{ww}}{z^2} \overset{*}{=} \frac{1}{2}\partial_z\partial_z(\gamma_{ww} - \gamma_{zz}) + \frac{-2\gamma_{xy}\partial_z\gamma_{xz}\partial_z\gamma_{yz} + \gamma_{xx}(\partial_z\gamma_{yz})^2 + \gamma_{yy}(\partial_z\gamma_{xz})^2}{\gamma_{xx}\gamma_{yy} - \gamma_{xy}^2}. \tag{A.21}$$

(6)

$$\frac{K_{iz} - \delta_{iz}K_{ww}}{z}$$

The division by z is again traded for a derivative if $i \neq z$ and for $i = z$, we use $K_{zz} = K_{ww} + \mathcal{O}(z^2)$, so that

$$\frac{K_{iz} - \delta_{iz}K_{ww}}{z} \overset{*}{=} \begin{cases} \partial_z K_{\hat{i}z} & \text{if } i = \hat{i} \\ 0 & \text{if } i = z \end{cases}. \tag{A.22}$$

Appendix B. Normalisation of the spatial normal frame vectors

In this section, we discuss how the set of spatial normal frame vectors, equation (4.38), can be recast in a form suitable for applying Gram–Schmidt orthonormalisation. It turns out to be convenient to first rescale the $\tilde{m}_{(\alpha)}$ such that they would acquire unit length in a flat spacetime with spatial metric δ_{IJ}. Denoting these rescaled vectors with a caret, we have

$$\hat{m}_{(\alpha)} = \frac{1}{\sqrt{\left(\sum_{s=\alpha}^{D-1} w_s^2\right)\left(\sum_{s=\alpha-1}^{D-1} w_s^2\right)}} \begin{pmatrix} \left.\begin{matrix} 0 \\ \vdots \\ 0 \end{matrix}\right\}(\alpha-2)\times \\ -\sum_{s=\alpha}^{D-1}(w^s)^2 \\ \left.\begin{matrix} w^{\alpha-1}w^{\alpha} \\ \vdots \\ w^{\alpha-1}w^{D-2} \\ w^{\alpha-1}w^{D-1} \end{matrix}\right\}(D-\alpha)\times \end{pmatrix}, \quad \alpha = 2, \ldots, D-1. \tag{B.1}$$

Recall that we formally set $w^1 \equiv x^1$, …, $w^{d-1} \equiv x^{d-1}$, $w^d \equiv z$. As a convenient shorthand, we define

$$\rho_I^2 \equiv \sum_{s=I}^{D-1} (w^s)^2, \tag{B.2}$$

so that, for instance, $\rho_1^2 = r^2$, $\rho_4^2 = (w^4)^2 + \ldots + (w^{D-1})^2$, $\rho_{D-1} = w^{D-1}$. This definition allows us to write

$$\hat{m}^I_{(\alpha)} = \frac{1}{\rho_\alpha\, \rho_{\alpha-1}} \begin{pmatrix} \left.\begin{matrix} 0 \\ \vdots \\ 0 \end{matrix}\right\}(\alpha-2)\times \\ -\rho_\alpha^2 \\ \left.\begin{matrix} w^{\alpha-1}w^\alpha \\ \vdots \\ w^{\alpha-1}w^{D-2} \\ w^{\alpha-1}w^{D-1} \end{matrix}\right\}(D-\alpha)\times \end{pmatrix}. \tag{B.3}$$

We can now express the angles ϕ^α in terms of the radial variables ρ_I,

$$\sin\phi^\alpha = \frac{\rho_\alpha}{\rho_{\alpha-1}}, \quad \cos\phi^\alpha = \frac{w^{\alpha-1}}{\rho_{\alpha-1}}. \tag{B.4}$$

Using these relations in (B.3), we obtain

$$\hat{m}^I_{(\alpha)} = \begin{pmatrix} \left.\begin{matrix} 0 \\ \vdots \\ 0 \end{matrix}\right\}(\alpha-2)\times \\ -\sin\phi^\alpha \\ \cos\phi^\alpha\, \cos\phi^{\alpha+1} \\ \cos\phi^\alpha\, \sin\phi^{\alpha+1}\, \cos\phi^{\alpha+2} \\ \vdots \\ \cos\phi^\alpha\, \sin\phi^{\alpha+1}\, \ldots\, \sin\phi^{D-2}\, \cos\phi^{D-1} \\ \cos\phi^\alpha\, \sin\phi^{\alpha+1}\, \ldots\, \sin\phi^{D-2}\, \sin\phi^{D-1} \end{pmatrix} = \begin{pmatrix} \left.\begin{matrix} 0 \\ \vdots \\ 0 \end{matrix}\right\}(\alpha-2)\times \\ -\sin\phi^\alpha \\ \vdots \\ \cos\phi^\alpha\Big(\prod_{s=\alpha+1}^{\alpha+n-1}\sin\phi^s\Big)\cos\phi^{\alpha+n} \\ \vdots \end{pmatrix}, \tag{B.5}$$

where $n = 1, \ldots, D-\alpha$, and we formally set $\cos\phi^{D-1} \equiv 1$ and $\prod_{s=\alpha+1}^{\alpha}\sin\phi^\alpha \equiv 1$.

Now, in our computational domain $\rho_{d+1}^2 = 0$, which, from the definition of our coordinate system in equation (2.8) gives

$$r^2 \sin^2\phi^2\, \ldots\, \sin^2\phi^{d+1} = 0 \tag{B.6}$$

Since $\phi^2, \ldots, \phi^d$ are arbitrary in our computational domain, we must have either $\phi^{d+1} = 0$ or π. Without loss of generality, we choose $\phi^{d+1} = 0$, which fixes the $d-1$ vectors

$$\hat{m}_{(2)} = (-\sin\phi^2,\ \cos\phi^2\cos\phi^3,\ \ldots,\ \cos\phi^2\prod_{s=3}^{d}\sin(\phi^s),\ \underbrace{0,\ \ldots,\ 0}_{(D-d-1)\times}). \tag{B.7}$$

$$\vdots$$

$$\hat{m}_{(\hat{\alpha})} = (\underbrace{0,\ \ldots,\ 0}_{(\hat{\alpha}-2)\times},\ -\sin\phi^{\hat{\alpha}},\ \cos\phi^{\hat{\alpha}}\cos\phi^{\hat{\alpha}+1},\ \ldots,\ \cos\phi^{\hat{\alpha}}\prod_{s=\hat{\alpha}+1}^{d}(\sin\phi^{s}),\ \underbrace{0,\ \ldots,\ 0}_{(D-d-1)\times}) \tag{B.8}$$

$$\vdots$$

$$\hat{m}_{(d)} = (\underbrace{0,\ \ldots,\ 0}_{(d-2)\times},\ -\sin\phi^{d},\ \cos\phi^{d},\ \underbrace{0,\ \ldots,\ 0}_{(D-d-1)\times}), \tag{B.9}$$

which, up to rescaling by $\rho_{\hat{\alpha}}\rho_{\hat{\alpha}-1}$, are equal to the vectors in equations (4.40)–(4.42). For the remaining vectors, we can use the rotational freedom in the angles ϕ^{d+2}, …, ϕ^{D-1}. Any choice for these values will satisfy $w^{d+1} = \ldots = w^{D-1} = 0$ as required on our computational domain and we merely need to ensure that we choose these angles such that the resulting set of vectors is orthogonal. This is most conveniently achieved by setting

$$\phi^{d+2} = \ldots = \phi^{D-1} = 0, \tag{B.10}$$

which, inserted into equation (B.5), implies

$$\hat{m}^{I}_{(a)} = \delta^{I}_{a}, \quad a = d+1, \ldots, D-1. \tag{B.11}$$

Combined with equations (B.7)–(B.9) and restoring the tilde in place of the caret on the $\tilde{m}_{(a)}$, we have recovered equations (4.43) and (4.44) in section 4.2 for the angular vectors. For the case $d = 3$ we have just two non-trivial vectors:

$$\hat{m}_{(2)} = (-\sin\phi^{2},\ \cos\phi^{2}\cos\phi^{3},\ \cos\phi^{2}\sin\phi^{3},\ \underbrace{0,\ \ldots,\ 0}_{(D-4)\times}), \tag{B.12}$$

$$\hat{m}_{(3)} = (0,\ -\sin\phi^{3},\ \cos\phi^{3},\ \underbrace{0,\ \ldots,\ 0}_{(D-4)\times}), \tag{B.13}$$

recovering equations (4.46)–(4.50).

References

[1] Godazgar M and Reall H S 2012 Peeling of the Weyl tensor and gravitational radiation in higher dimensions *Phys. Rev.* D **85** 084021
[2] Abbott B P *et al* 2016 Observation of gravitational waves from a binary black hole merger *Phys. Rev. Lett.* **116** 061102
[3] Abbott B P *et al* 2016 GW151226: observation of gravitational waves from a 22-solar-mass binary black hole coalescence *Phys. Rev. Lett.* **116** 241103
[4] Abbott B P *et al* 2016 Properties of the binary black hole merger GW150914 *Phys. Rev. Lett.* **116** 241102
[5] Abbott B P *et al* 2016 Directly comparing GW150914 with numerical solutions of Einstein's equations for binary black hole coalescence *Phys. Rev.* D **94** 064035
[6] Abbott B P *et al* 2016 Tests of general relativity with GW150914 *Phys. Rev. Lett.* **116** 221101
[7] Abbott B P *et al* 2016 Astrophysical implications of the binary black-hole merger GW150914 *Astrophys. J.* **818** L22
[8] Adrian-Martinez S *et al* 2016 High-energy neutrino follow-up search of gravitational wave event GW150914 with ANTARES and IceCube *Phys. Rev.* D **93** 122010
[9] Regge T and Wheeler J A 1957 Stability of a Schwarzschild singularity *Phys. Rev.* **108** 1063–9
[10] Zerilli F J 1970 Effective potential for even parity Regge-Wheeler gravitational perturbation equations *Phys. Rev. Lett.* **24** 737–8

[11] Emparan R and Reall H S 2008 Black holes in higher dimensions *Living Rev. Relativ.* vol **11** p 1
[12] Figueras P, Kunesch M and Tunyasuvunakool S 2015 The endpoint of black ring instabilities and the weak cosmic censorship conjecture *Phys. Rev. Lett.* **116** 071102
[13] Shibata M and Yoshino H 2010 Bar-mode instability of rapidly spinning black hole in higher dimensions: numerical simulation in general relativity *Phys. Rev.* D **81** 104035
[14] Santos J E and Way B 2015 Neutral black rings in five dimensions are unstable *Phys. Rev. Lett.* **114** 221101
[15] Zilhão M, Cardoso V, Herdeiro C, Lehner L and Sperhake U 2014 Testing the nonlinear stability of Kerr-Newman black holes *Phys. Rev.* D **90** 124088
[16] Dafermos M and Rodnianski I 2010 The black hole stability problem for linear scalar perturbations *On Recent Developments in Theoretical and Experimental General Relativity, Astrophysics and Relativistic Field Theories. Proc., 12th Marcel Grossmann Meeting on General Relativity (Paris, France, 12–18 July 2009) vol* 1–3 pp 132–89
[17] Kanti P 2009 Black holes at the LHC *Lect. Notes Phys.* **769** 387–423
[18] Cardoso V, Gualtieri L, Herdeiro C and Sperhake U 2015 Exploring new physics frontiers through numerical relativity *Living Rev. Relativ.* **18** 1
[19] Choptuik M W, Lehner L and Pretorius F 2015 Probing strong field gravity through numerical simulations (arXiv:1502.06853 [gr-qc])
[20] Bondi H, Pirani F A E and Robinson I 1959 Gravitational waves in general relativity. 3. Exact plane waves *Proc. R. Soc.* A **251** 519–33
[21] Pirani F A E 1957 Invariant formulation of gravitational radiation theory *Phys. Rev.* **105** 1089–99
[22] Bondi H 1957 Plane gravitational waves in general relativity *Nature* **179** 1072–3
[23] Bondi H 1960 Gravitational waves in general relativity *Nature* **186** 535
[24] Newman E and Penrose R 1962 An approach to gravitational radiation by a method of spin coefficients *J. Math. Phys.* **3** 566–78
[25] Bondi H, van der Burg M G J and Metzner A W K 1962 Gravitational waves in general relativity VII. Waves from axisymmetric isolated systems *Proc. R. Soc.* A **269** 21–52
[26] Sachs R K 1962 Gravitational waves in general relativity. 8. Waves in asymptotically flat space-times *Proc. R. Soc.* A **270** 103–26
[27] Saulson P R 2011 Josh Goldberg and the physical reality of gravitational waves *Gen. Relativ. Gravit.* **43** 3289–99
[28] Peters P C 1964 Gravitational radiation and the motion of two point masses *Phys. Rev.* **136** B1224–32
[29] Cunningham C T, Price R H and Moncrief V 1978 Radiation from collapsing relativistic stars. I. Linearized odd-parity radiation *Astrophys. J.* **224** 643–67
[30] Cunningham C T, Price R H and Moncrief V 1979 Radiation from collapsing relativistic stars. II. Linearized even parity radiation *Astrophys. J.* **230** 870–92
[31] Blanchet L, Damour T and Schaefer G 1990 Post-Newtonian hydrodynamics and post-Newtonian gravitational wave generation for numerical relativity *Mon. Not. R. Astron. Soc.* **242** 289–305
[32] Blanchet L, Damour T, Iyer B R, Will C M and Wiseman A G 1995 Gravitational-radiation damping of compact binary systems to second post-Newtonian order *Phys. Rev. Lett.* **74** 3515–8
[33] Ruiz M, Takahashi R, Alcubierre M and Nuñez D 2008 Multipole expansions for energy and momenta carried by gravitational waves *Gen. Relativ. Gravit.* **40** 1705–29
[34] Nerozzi A and Elbracht O 2008 Using curvature invariants for wave extraction in numerical relativity (arXiv:0811.1600 [gr-qc])
[35] Centrella J M, Baker J G, Kelly B J and van Meter J R 2010 Black-hole binaries, gravitational waves, and numerical relativity *Rev. Mod. Phys.* **82** 3069
[36] Reisswig C, Ott C D, Sperhake U and Schnetter E 2011 Gravitational wave extraction in simulations of rotating stellar core collapse *Phys. Rev.* D **83** 064008
[37] Hinder I *et al* 2014 Error-analysis and comparison to analytical models of numerical waveforms produced by the NRAR Collaboration *Class. Quantum Grav.* **31** 025012
[38] Lehner L and Moreschi O M 2007 Dealing with delicate issues in waveform calculations *Phys. Rev.* D **76** 124040
[39] Read J S *et al* 2013 Matter effects on binary neutron star waveforms *Phys. Rev.* D **88** 044042
[40] Mroué A H *et al* 2013 A catalog of 171 high-quality binary black-hole simulations for gravitational-wave astronomy *Phys. Rev. Lett.* **111** 241104
[41] Taracchini A *et al* 2014 Effective-one-body model for black-hole binaries with generic mass ratios and spins *Phys. Rev.* D **89** 061502

[42] Pürrer M 2014 Frequency domain reduced order models for gravitational waves from aligned-spin compact binaries *Class. Quantum Grav.* **31** 195010
[43] Khan S *et al* 2016 Frequency-domain gravitational waves from non-precessing black-hole binaries. II. A phenomenological model for the advanced detector era *Phys. Rev.* D **93** 044007
[44] Hannam M *et al* 2014 A simple model of complete precessing black-hole-binary gravitational waveforms *Phys. Rev. Lett.* **113** 151101
[45] Moncrief V 1974 Gravitational perturbations of spherically symmetric systems. I. The exterior problem *Ann. Phys.* **88** 323–42
[46] Thorne K S 1980 Multipole expansions of gravitational radiation *Rev. Mod. Phys.* **52** 299–339
[47] Ott C D, Dimmelmeier H, Marek A, Janka H-T, Hawke I, Zink B and Schnetter E 2007 3D collapse of rotating stellar iron cores in general relativity with microphysics *Phys. Rev. Lett.* **98** 261101
[48] Shibata M and Sekiguchi Y-I 2005 Three-dimensional simulations of stellar core collapse in full general relativity: nonaxisymmetric dynamical instabilities *Phys. Rev.* D **71** 024014
[49] Landau L D and Lifshitz E M 1975 The classical theory of fields (Oxford: Elsevier)
[50] Lovelace G, Chen Y, Cohen M, Kaplan J D, Keppel D, Matthews K D, Nichols D A, Scheel M A and Sperhake U 2010 Momentum flow in black-hole binaries. II. Numerical simulations of equal-mass, head-on mergers with antiparallel spins *Phys. Rev.* D **82** 064031
[51] Reisswig C, Bishop N T, Pollney D and Szilagyi B 2009 Unambiguous determination of gravitational waveforms from binary black hole mergers *Phys. Rev. Lett.* **103** 221101
[52] Reisswig C, Bishop N T, Pollney D and Szilagyi B 2010 Characteristic extraction in numerical relativity: binary black hole merger waveforms at null infinity *Class. Quantum Grav.* **27** 075014
[53] Babiuc M C, Szilagyi B, Winicour J and Zlochower Y 2011 A characteristic extraction tool for gravitational waveforms *Phys. Rev.* D **84** 044057
[54] Pretorius F 2005 Evolution of binary black hole spacetimes *Phys. Rev. Lett.* **95** 121101
[55] Baker J G, Centrella J, Choi D-I, Koppitz M and van Meter J 2006 Gravitational-wave extraction from an inspiraling configuration of merging black holes *Phys. Rev. Lett.* **96** 111102
[56] Campanelli M, Lousto C O, Marronetti P and Zlochower Y 2006 Accurate evolutions of orbiting black-hole binaries without excision *Phys. Rev. Lett.* **96** 111101
[57] Sperhake U 2007 Binary black-hole evolutions of excision and puncture data *Phys. Rev.* D **76** 104015
[58] Herrmann F, Hinder I, Shoemaker D, Laguna P and Matzner R A 2007 Gravitational recoil from spinning binary black hole mergers *Astrophys. J.* **661** 430–6
[59] Brügmann B, González J A, Hannam M D, Husa S, Sperhake U and Tichy W 2008 Calibration of moving puncture simulations *Phys. Rev.* D **77** 024027
[60] Boyle M, Brown D A, Kidder L E, Mroué A H, Pfeiffer H P, Scheel M A, Cook G B and Teukolsky S A 2007 High-accuracy comparison of numerical relativity simulations with post-Newtonian expansions *Phys. Rev.* D **76** 124038
[61] Bishop N T and Rezzolla L 2016 Extraction of gravitational waves in numerical relativity *Living Rev. Relativ.* **20** 1
[62] Cardoso V, Dias O J C and Lemos J P S 2003 Gravitational radiation in D-dimensional space-times *Phys. Rev.* D **67** 064026
[63] Yoshino H and Shibata M 2009 Higher-dimensional numerical relativity: formulation and code tests *Phys. Rev.* D **80** 084025
[64] Kodama H and Ishibashi A 2003 A master equation for gravitational perturbations of maximally symmetric black holes in higher dimensions *Prog. Theor. Phys.* **110** 701–22
[65] Ishibashi A and Kodama H 2011 Perturbations and stability of static black holes in higher dimensions *Prog. Theor. Phys. Suppl.* **189** 165–209
[66] Witek H, Zilhão M, Gualtieri L, Cardoso V, Herdeiro C, Nerozzi A and Sperhake U 2010 Numerical relativity for D dimensional space-times: head-on collisions of black holes and gravitational wave extraction *Phys. Rev.* D **82** 104014
[67] Witek H, Cardoso V, Gualtieri L, Herdeiro C, Sperhake U and Zilhao M 2011 Numerical relativity in *D* dimensional space-times: collisions of unequal mass black holes *J. Phys.: Conf. Ser.* **314** 012104
[68] Tangherlini F R 1963 Schwarzschild field in n dimensions and the dimensionality of space problem *Nuovo Cimento* **27** 636–51
[69] Witek H, Okawa H, Cardoso V, Gualtieri L, Herdeiro C, Shibata M, Sperhake U and Zilhão M 2014 Higher dimensional numerical relativity: code comparison *Phys. Rev.* D **90** 084014

[70] Ortaggio M, Pravda V, Pravdova A and Reall H S 2012 On a five-dimensional version of the Goldberg-Sachs theorem *Class. Quantum Grav.* **29** 205002
[71] Teukolsky S A 1972 Rotating black holes—separable wave equations for gravitational and electromagnetic perturbations *Phys. Rev. Lett.* **29** 1114–8
[72] Teukolsky S A 1973 Perturbations of a rotating black hole. 1. Fundamental equations for gravitational electromagnetic and neutrino field perturbations *Astrophys. J.* **185** 635–47
[73] Durkee M and Reall H S 2011 Perturbations of higher-dimensional spacetimes *Class. Quantum Grav.* **28** 035011
[74] Chesler P M and Yaffe L G 2014 Numerical solution of gravitational dynamics in asymptotically anti-de Sitter spacetimes *J. High Energy Phys.* JHEP07(2014)086
[75] Zilhao M, Witek H, Sperhake U, Cardoso V, Gualtieri L, Herdeiro C and Nerozzi A 2010 Numerical relativity in higher dimensions *J. Phys.: Conf. Ser.* **229** 012074
[76] Zilhao M 2012 New frontiers in numerical relativity *PhD Thesis* Aveiro University
[77] Pretorius F 2005 Numerical relativity using a generalized harmonic decomposition *Class. Quantum Grav.* **22** 425–52
[78] Shibata M and Yoshino H 2010 Nonaxisymmetric instability of rapidly rotating black hole in five dimensions *Phys. Rev.* D **81** 021501
[79] Yoshino H and Shibata M 2011 Higher-dimensional numerical relativity: current status *Prog. Theor. Phys. Suppl.* **189** 269–310
[80] Yoshino H and Shibata M 2011 Exploring higher-dimensional black holes in numerical relativity *Prog. Theor. Phys. Suppl.* **190** 282–303
[81] Shibata M and Nakamura T 1995 Evolution of three-dimensional gravitational waves: harmonic slicing case *Phys. Rev.* D **52** 5428–44
[82] Baumgarte T W and Shapiro S L 1998 On the numerical integration of Einstein's field equations *Phys. Rev.* D **59** 024007
[83] Cook W G, Figueras P, Kunesch M, Sperhake U and Tunyasuvunakool S 2016 Dimensional reduction in numerical relativity: modified cartoon formalism and regularization *3rd Amazonian Symp. on Physics and 5th NRHEP Network Meeting: Celebrating 100 Years of General Relativity (Belem, Brazil, 28 September–2 October 2015) Int. J. Mod. Phys.* D **25** 1641013
[84] Arnowitt R, Deser S and Misner C W 1962 The dynamics of general relativity *Gravitation an Introduction to Current Research* ed L Witten (New York: Wiley) pp 227–65
[85] Misner C W, Thorne K S and Wheeler J A 1973 *Gravitation* (New York: W. H. Freeman)
[86] York J W Jr 1979 Kinematics and dynamics of general relativity *Sources of Gravitational Radiation* ed L Smarr (Cambridge: Cambridge University Press) pp 83–126
[87] Gourgoulhon E 2007 3 + 1 formalism and bases of numerical relativity (arXiv: gr-qc/0703035)
[88] Sperhake U 2013 Black holes on supercomputers: numerical relativity applications to astrophysics and high-energy physics *Acta Phys. Pol.* B **44** 2463–536
[89] Cao Z and Hilditch D 2012 Numerical stability of the Z4c formulation of general relativity *Phys. Rev.* D **85** 124032
[90] Alic D, Bona-Casas C, Bona C, Rezzolla L and Palenzuela C 2012 Conformal and covariant formulation of the Z4 system with constraint-violation damping *Phys. Rev.* D **85** 064040
[91] Hilditch D, Bernuzzi S, Thierfelder M, Cao Z, Tichy W and Brügmann B 2013 Compact binary evolutions with the Z4c formulation *Phys. Rev.* D **88** 084057
[92] Garfinkle D 2002 Harmonic coordinate method for simulating generic singularities *Phys. Rev.* D **65** 044029
[93] Alcubierre M, Brandt S, Bruegmann B, Holz D, Seidel E, Takahashi R and Thornburg J 2001 Symmetry without symmetry: numerical simulation of axisymmetric systems using Cartesian grids *Int. J. Mod. Phys.* D **10** 273–90
[94] Tanabe K, Kinoshita S and Shiromizu T 2011 Asymptotic flatness at null infinity in arbitrary dimensions *Phys. Rev.* D **84** 044055
[95] Kinnersley W 1969 Type D vacuum metrics *J. Math. Phys.* **10** 1195–203
[96] Zhang F, Brink J, Szilagyi B and Lovelace G 2012 A geometrically motivated coordinate system for exploring spacetime dynamics in numerical-relativity simulations using a quasi-Kinnersley tetrad *Phys. Rev.* D **86** 084020
[97] Sperhake U, Berti E, Cardoso V, Gonzalez J A, Bruegmann B and Ansorg M 2008 Eccentric binary black-hole mergers: the transition from inspiral to plunge in general relativity *Phys. Rev.* D **78** 064069
[98] Cactus Computational Toolkit homepage: http://cactuscode.org/

[99] Allen G, Goodale T, Massó J and Seidel E 1999 The cactus computational toolkit and using distributed computing to collide neutron stars *Proc. of 8th IEEE Int. Symp. on High Performance Distributed Computing (Redondo Beach, 1999) (*IEEE Press)
[100] Carpet Code homepage: http://carpetcode.org/
[101] Schnetter E, Hawley S H and Hawke I 2004 Evolutions in 3D numerical relativity using fixed mesh refinement *Class. Quantum Grav.* **21** 1465–88
[102] van Meter J R, Baker J G, Koppitz M and Choi D-I 2006 How to move a black hole without excision: gauge conditions for the numerical evolution of a moving puncture *Phys. Rev.* D **73** 124011
[103] Brill D R and Lindquist R W 1963 Interaction energy in geometrostatics *Phys. Rev.* **131** 471–6
[104] Zilhão M, Ansorg M, Cardoso V, Gualtieri L, Herdeiro C, Sperhake U and Witek H 2011 Higher-dimensional puncture initial data *Phys. Rev.* D **84** 084039